

Evaluation of Supernova Model Discrimination and Pointing Accuracy with SK-Gd

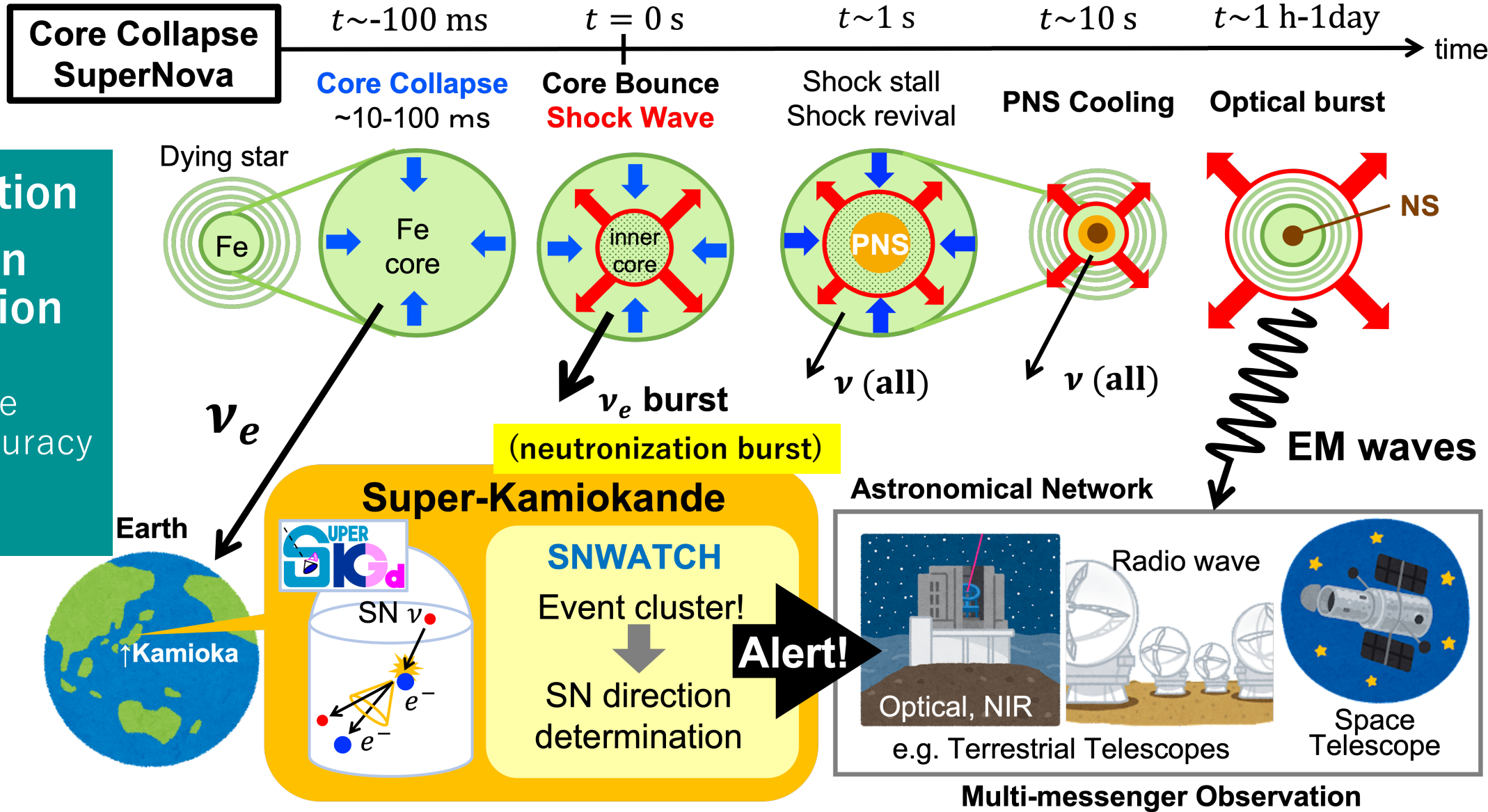
Yuri Kashiwagi (M2)
ICRR, Kamioka, Sekiya Lab.

Outline

- Introduction and Motivation
 - SK-Gd Project (2020-)
 - Supernova neutrino detection with SK-Gd
- Algorithm
 - SN direction determination with SK-Gd
 - Pointing accuracy derivation
- Method
 - Supernova models
 - Realistic supernova simulation in SK
 - Data format unification
- Results (6 supernova models)
 - SK's response for supernova at 10kpc with neutrino oscillation in NMO
 - Pointing accuracy for supernova at 10kpc
- Summary and Prospects

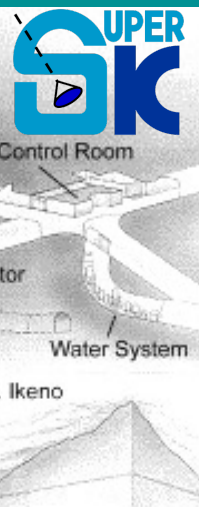
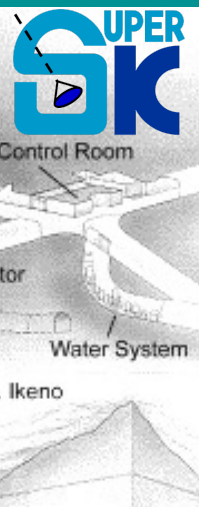
Vital role of SK in Supernova (SN) Observation

- SN ν detection
- SN direction determination
with the best possible pointing accuracy
- Alert issue



SK-Gd Project (2020-)

Fukuda, S., et al. *Nucl. Instrum. Methods Phys. Res. A* 501.2-3 (2003): 418-462.

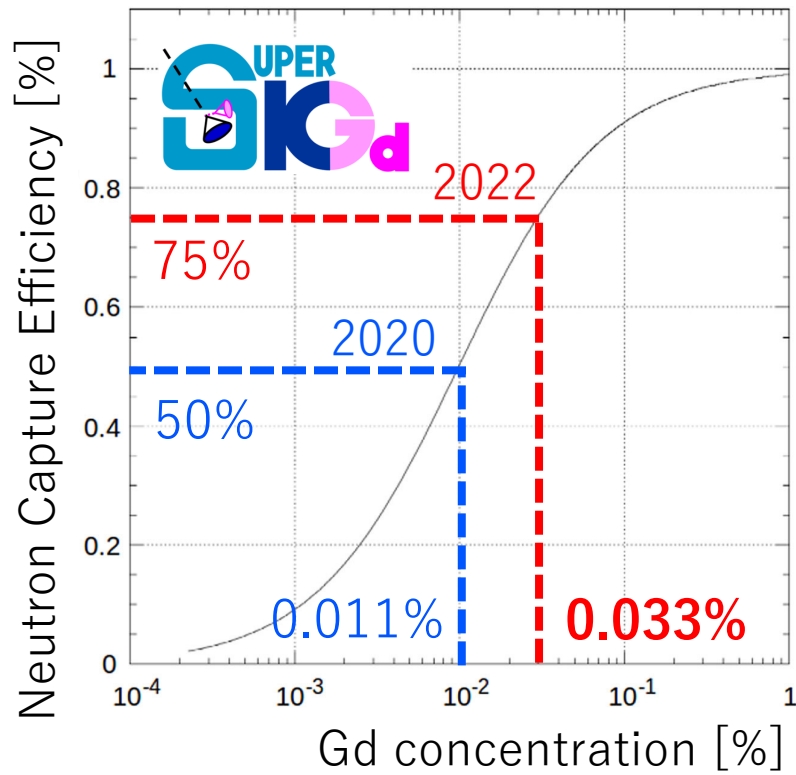
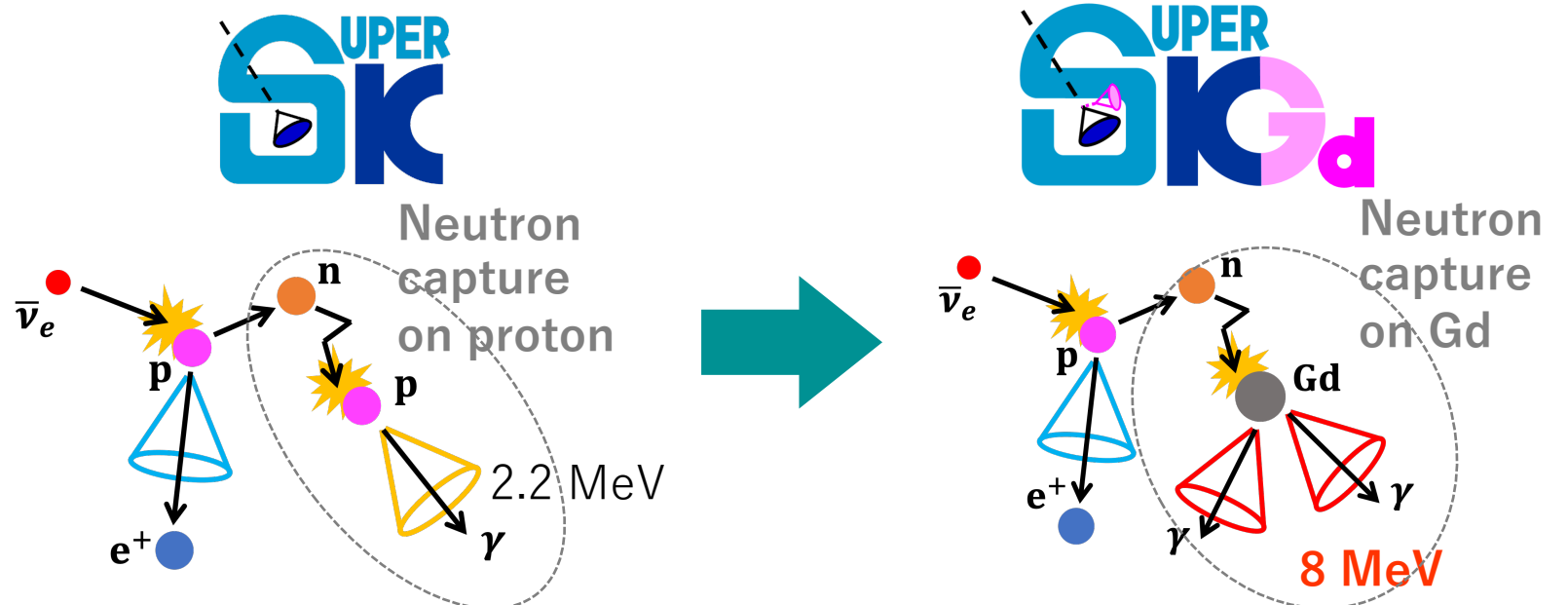


◆Gadolinium loading to SK water

Beacom & Vagins.
PRL 93 (2004) 171101

For enhancing neutron detection efficiency

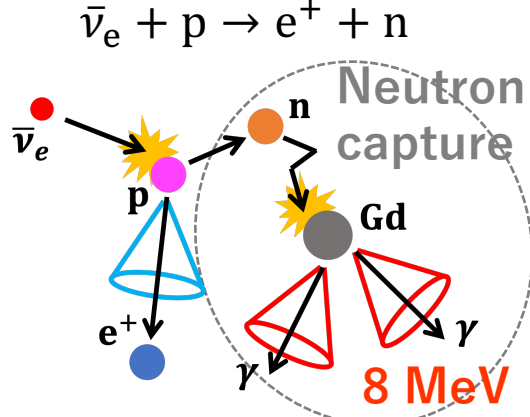
- easier to distinguish events with/without neutron capture
- better to determine supernova direction



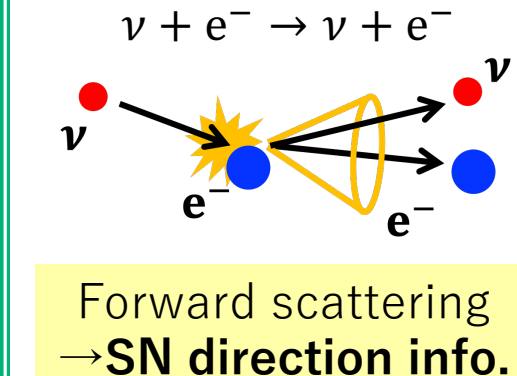
SN ν observation @ SK (\sim 5-30 MeV)

◆ Interactions between SN ν and SK water

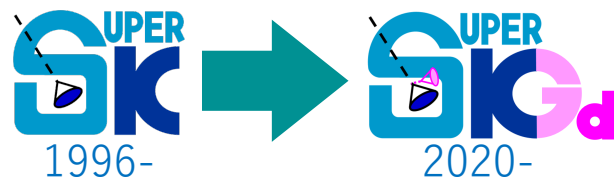
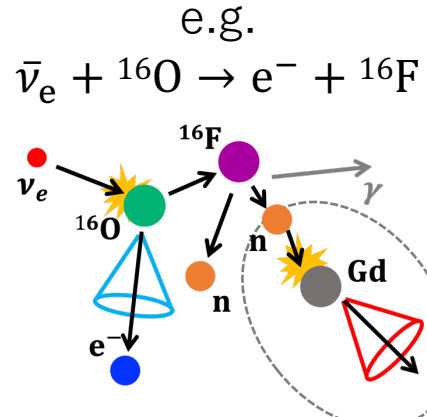
Inverse Beta Decay (IBD)



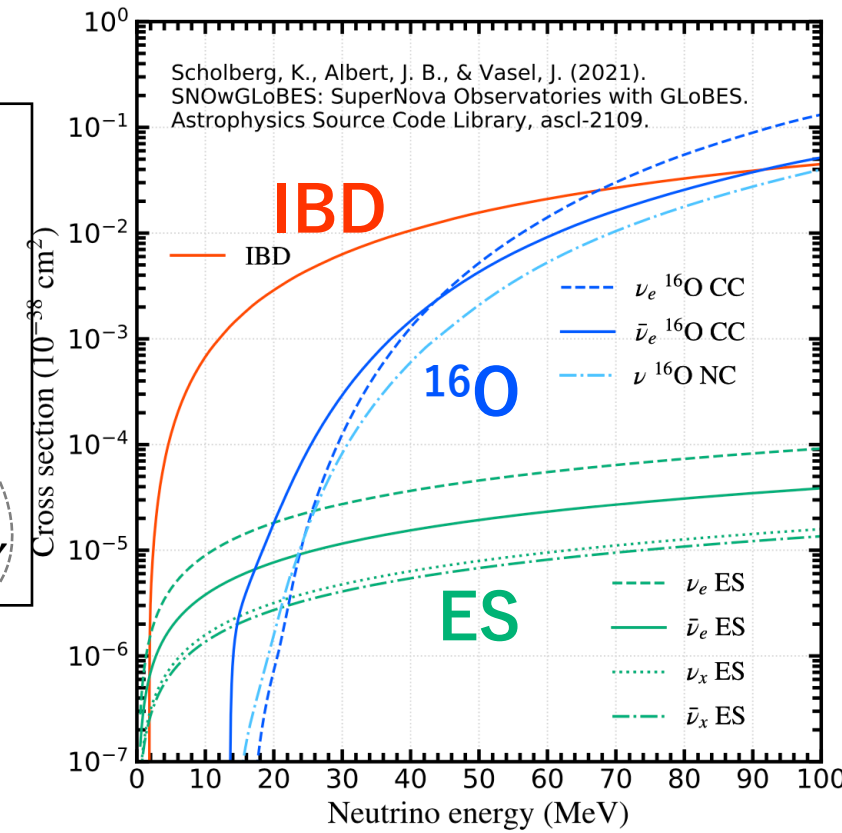
Elastic Scattering (ES)



^{16}O interactions



easier to distinguish IBD and ES
→ better pointing accuracy



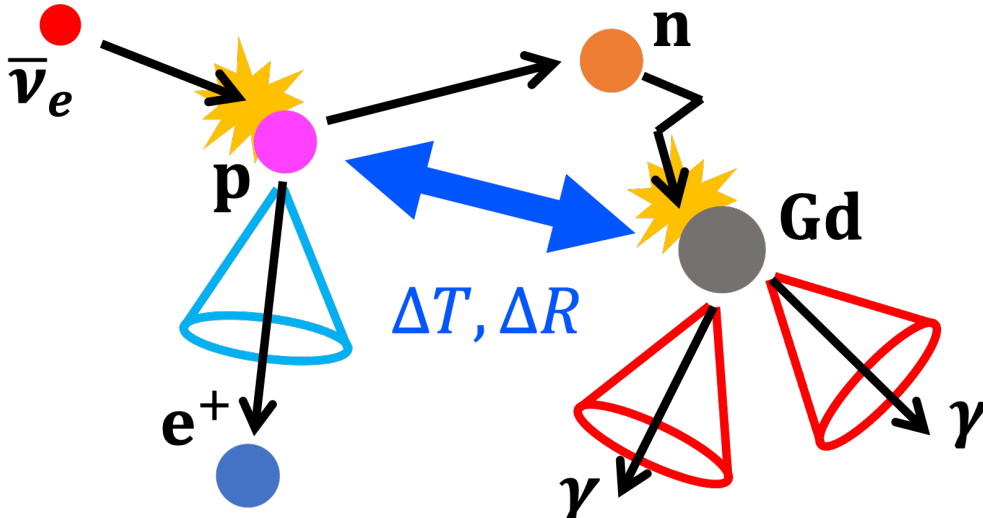
Cross section vs. Neutrino energy

◆ Motivation

- Understanding the Gd-loaded SK's response for various SN models
- Investigating whether SK-Gd achieves the goal of pointing SN within 3° accuracy

Event Selection and Neutron tagging in SNWATCH

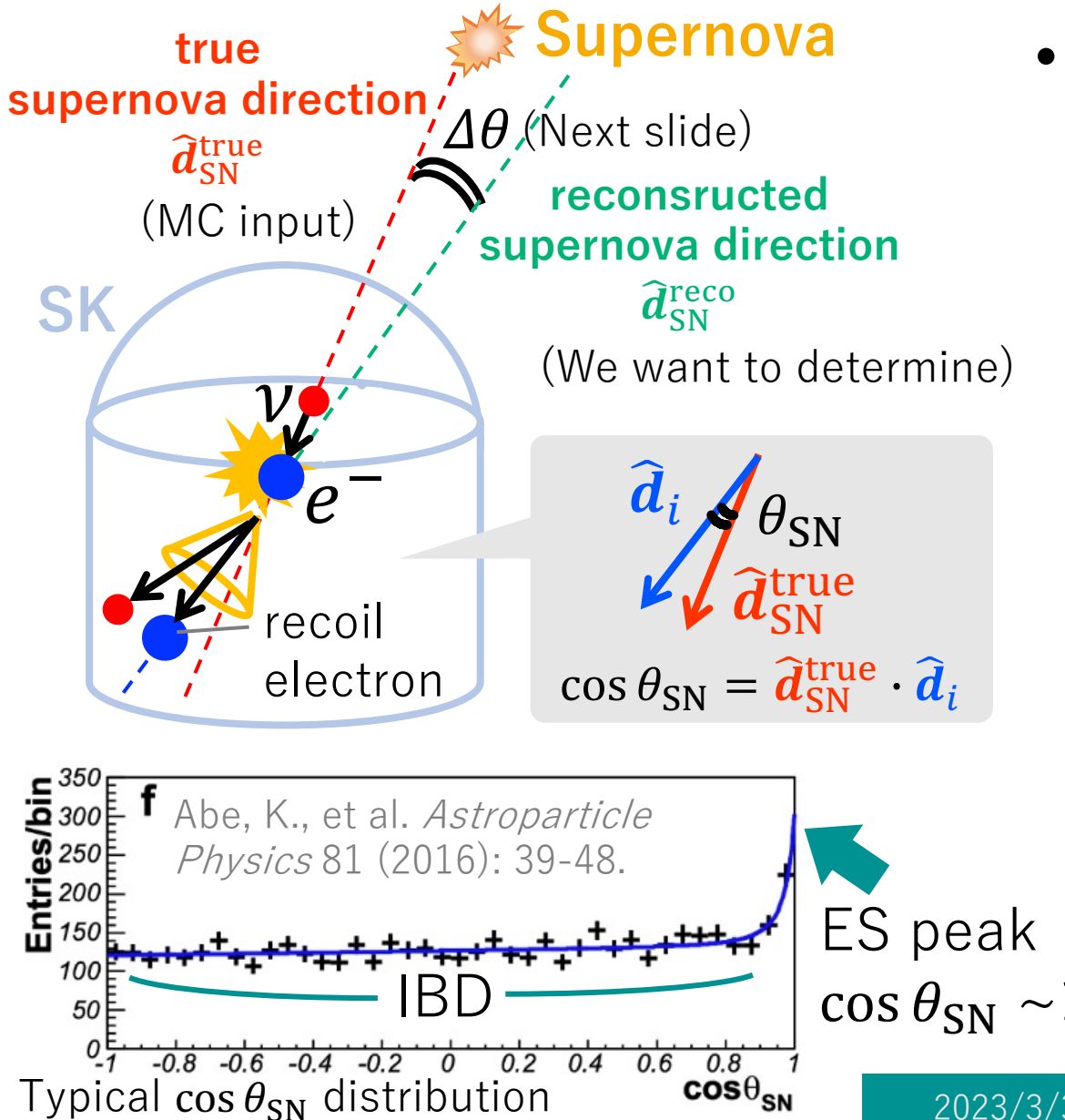
prompt candidates



delayed candidates

- To extract ES events:
Neutron tagging to identify IBD
- A speed-oriented simple algorithm
 - ① Selection of **prompt candidates** $\geq 7\text{ MeV}$
 - ② Selection of **delayed candidates**
 - ③ **Neutron tagging**
pair of events with
 $\Delta T < 500\text{ }\mu\text{s}$ & $\Delta R < 300\text{ cm}$

Determination of Supernova Direction in SNWATCH



- Maximum Likelihood Fit
 - The likelihood function for the i -th event

$$L_i = \sum_r N_{r,k} t_r(f_i) p_r(E_i, \hat{d}_i; \hat{d}_{SN}^{reco})$$

of event
 reaction (IBD, ES, ^{16}O CC)
 energy bin
 energy

tagging efficiency term

PDF function (determined by SK MC)

- Likelihood

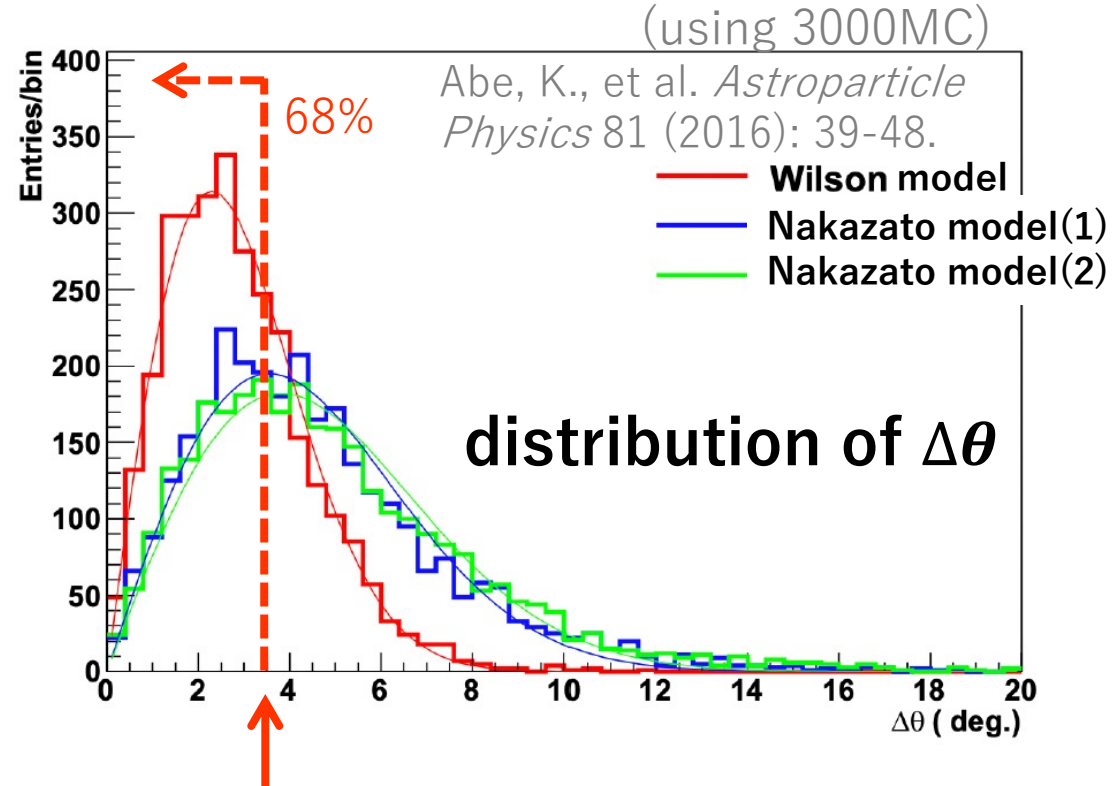
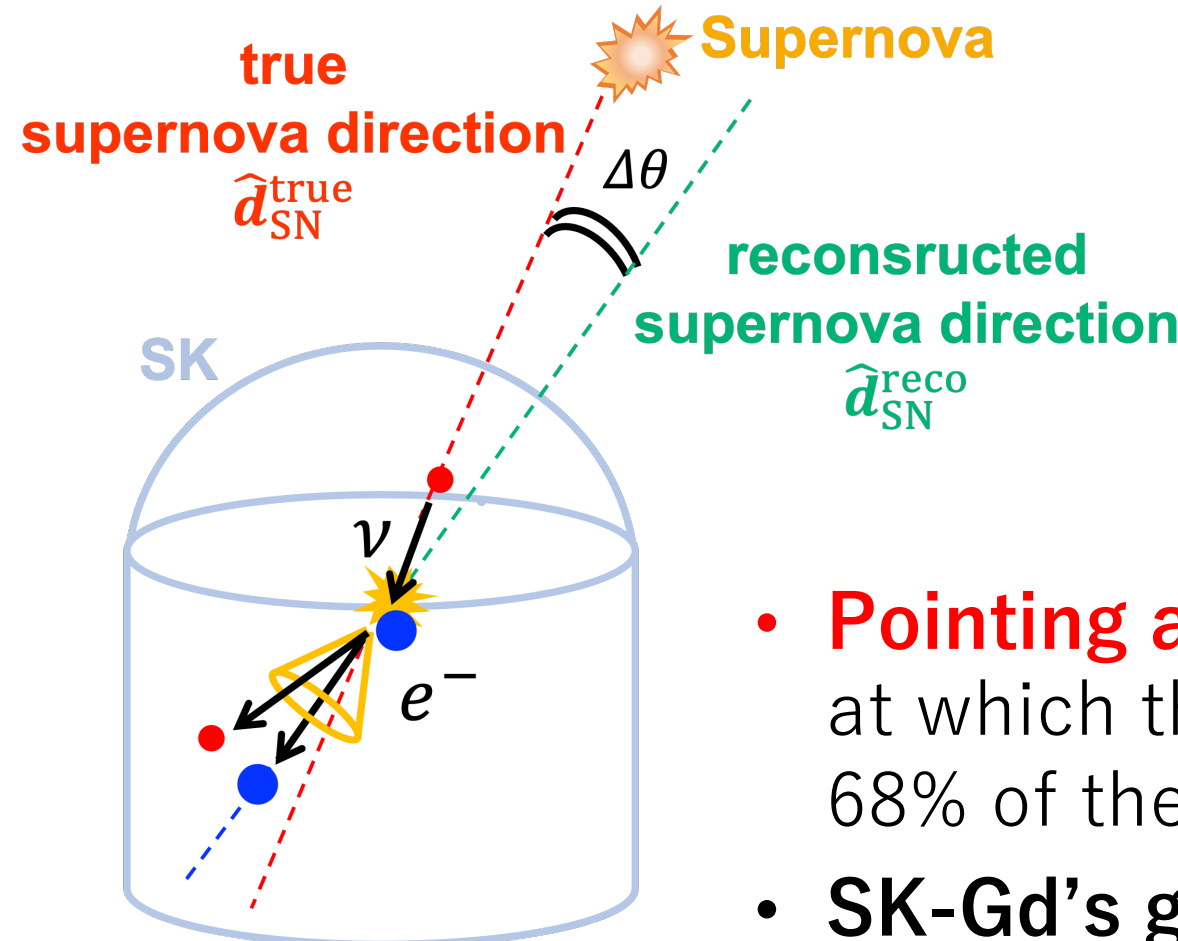
$$\mathcal{L} = \exp \left\{ \sum_{k,r} N_{r,k} \right\} \prod_i L_i$$

- Maximized by

$$\frac{\partial \mathcal{L}}{\partial N_{r,k}} = \frac{\partial \mathcal{L}}{\partial \hat{d}_{SN}^{reco}} = 0$$

Pointing Accuracy in SNWATCH

- Derived by $\Delta\theta$ distribution
 $\cos(\Delta\theta) = \hat{d}_{\text{SN}}^{\text{true}} \cdot \hat{d}_{\text{SN}}^{\text{reco}}$



- Pointing accuracy at 1σ** is the value of $\Delta\theta$ at which the integral of the histogram includes 68% of the 1000 MC samples
- SK-Gd's goal: 3° accuracy (Wilson model)**

Supernova Models

- Five 1D models + one 3D model
- After the data format unification

* Equation of state by Shen et al. (1998a, 1998b) [82, 83].

** Equation of state based on density-dependent relativistic mean-field model [98].

*** Equation of state by Lattimer and Swesty [96]

Summary of Supernova models. Core bounce occurs at 0 s.

Model Name	Wilson ^[1]	Nakazato ^[2]	Mori ^[3]	Hüdepohl ^[4]	Fischer ^[5]	Tamborra ^[6]
Dimension	1D	1D	1D	1D	1D	3D
progenitor mass [M_{\odot}]	20	20	9.6	8.8	8.8	27
start time [s]	0.03	-0.05	-0.256	-0.02	0.0	0.011
duration [s]	14.96	20.05	19.95	8.98	6.10	0.54
EoS	-	Shen*	DD2**	Shen*	Shen*	LS***

Reference

- [1] Totani, T., et al. *ApJ* 496.1 (1998): 216
- [2] Nakazato, K., et al. *ApJS* 205.1 (2013): 2
- [3] Mori, M., et al. *PTEP* 2021.2 (2021): 023E01
- [4] Hüdepohl, L., et al. *PhRvL* 104.25 (2010): 251101
- [5] Fischer, T., et al. *A&A* 517 (2010): A80
- [6] Tamborra et al. *PRD* 90.4 (2014): 045032.

SASI
 (Standing
 Accretion-Shock
 Instability)

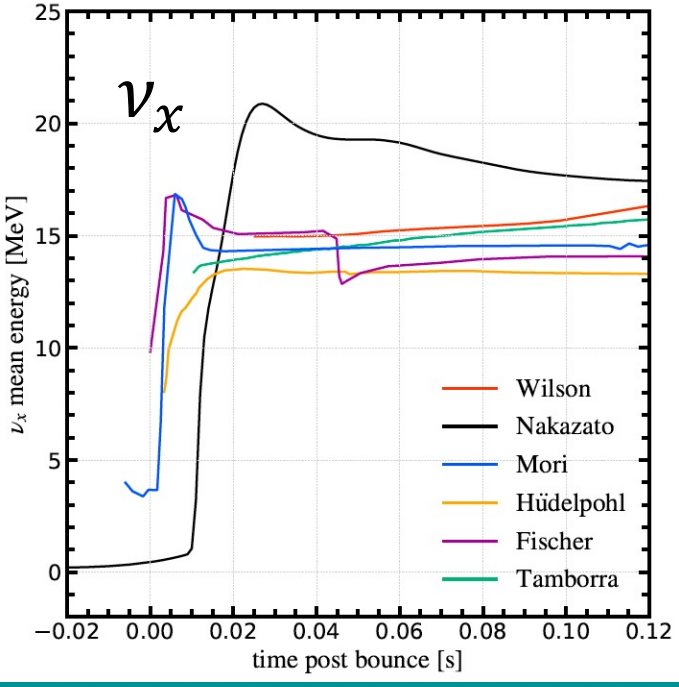
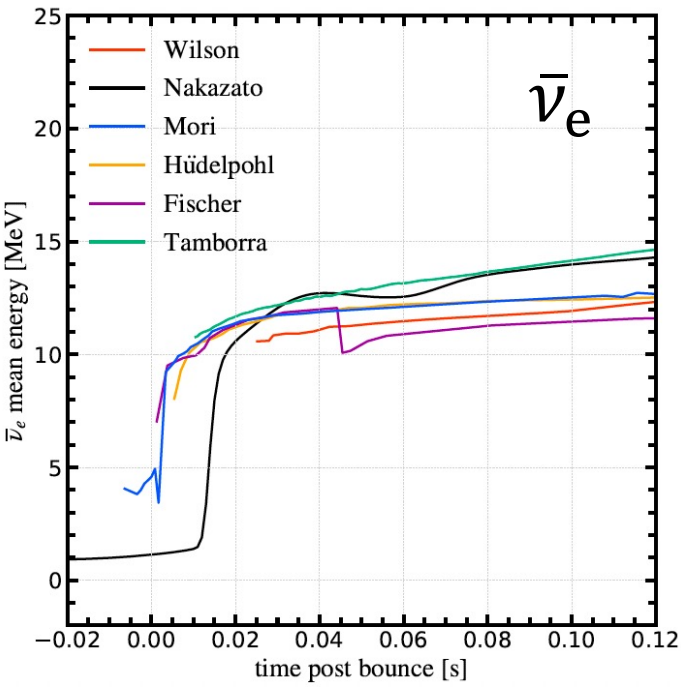
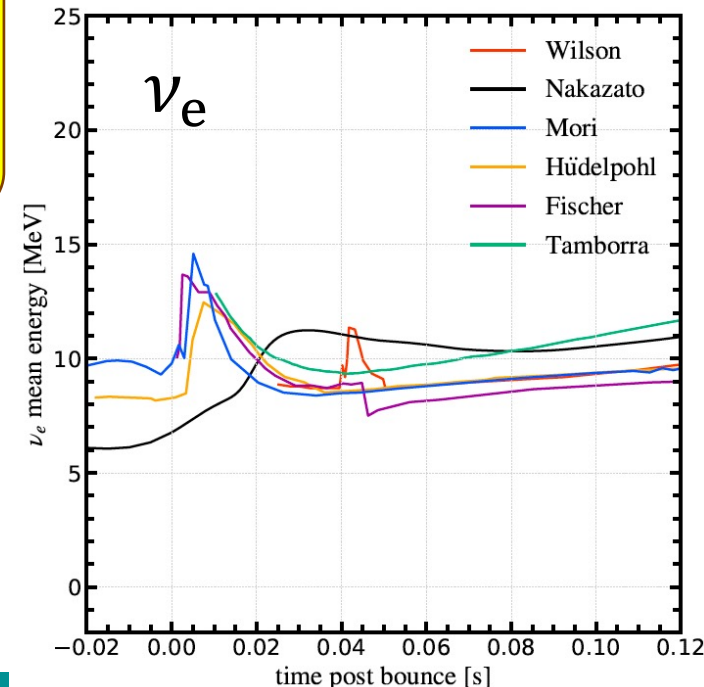
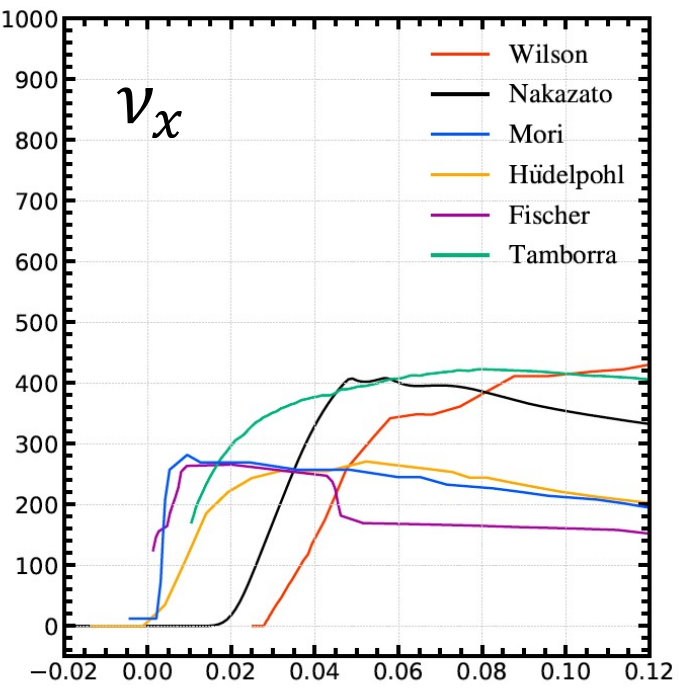
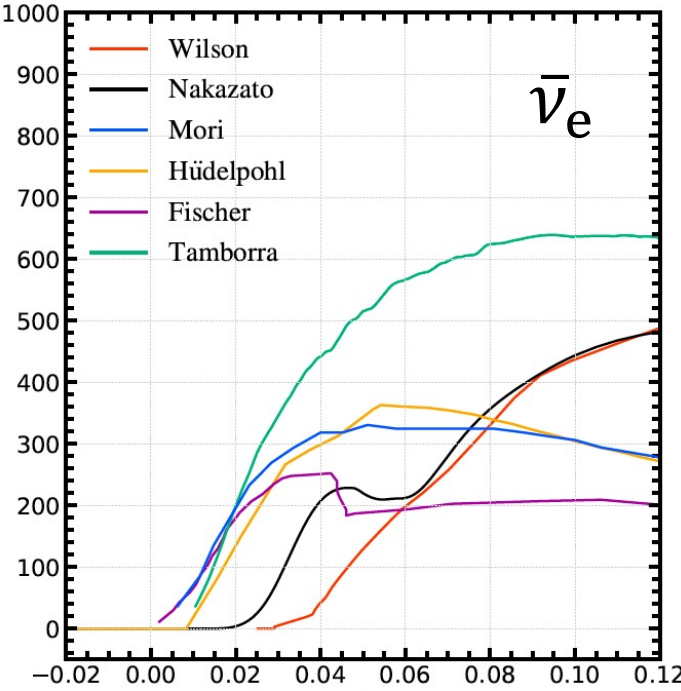
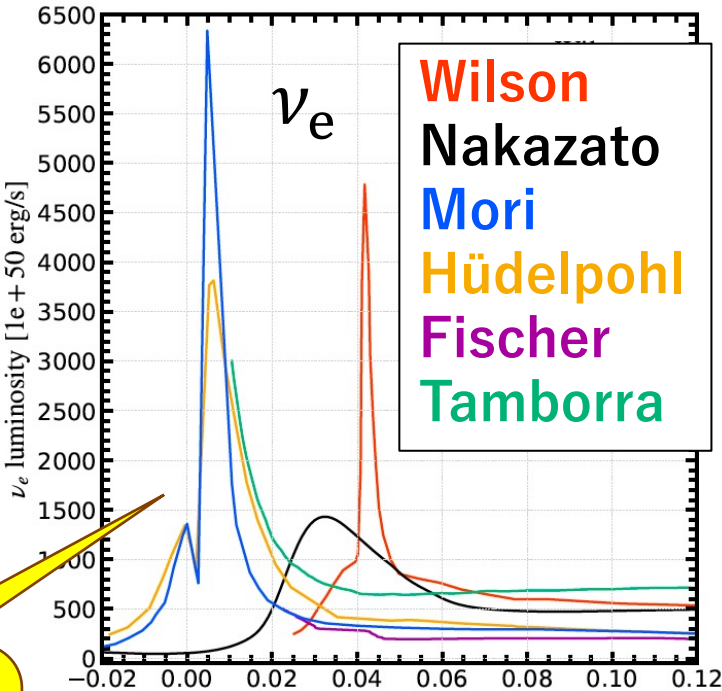
Electron capture
 Supernova
 (O-Ne-Mg core)

Method
6 models
until 0.12s

Luminosity
vs. time

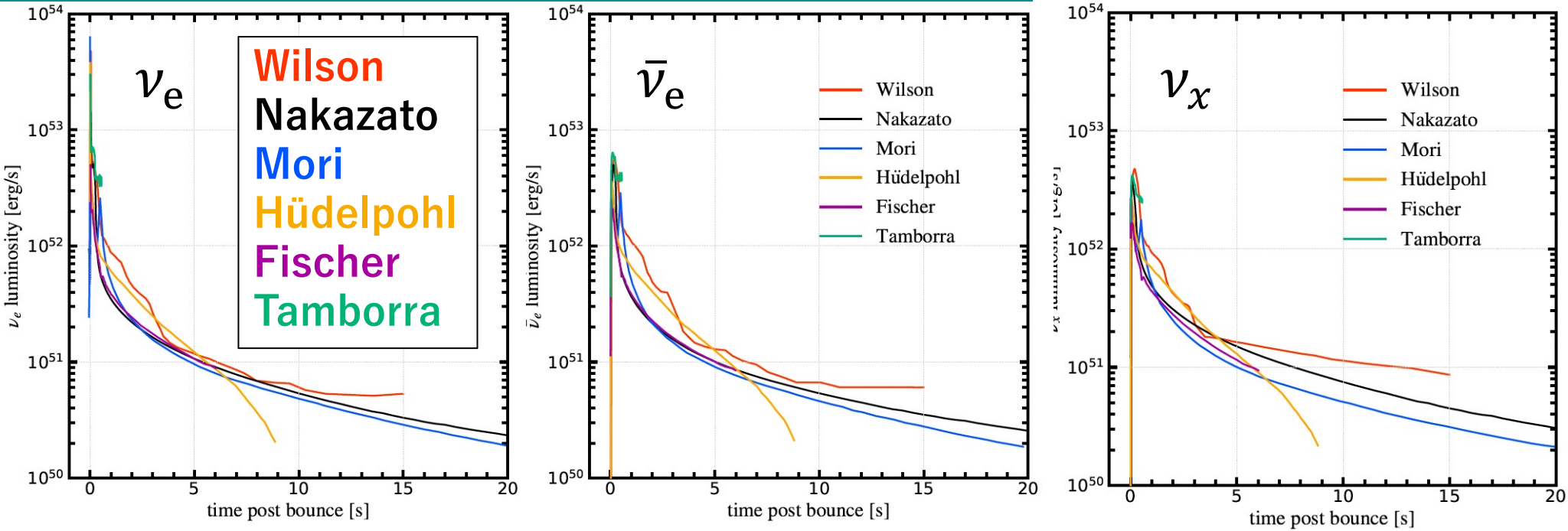
Neutronization
burst
(ν_e burst ≤ 0.1 s)

Mean energy
vs. time

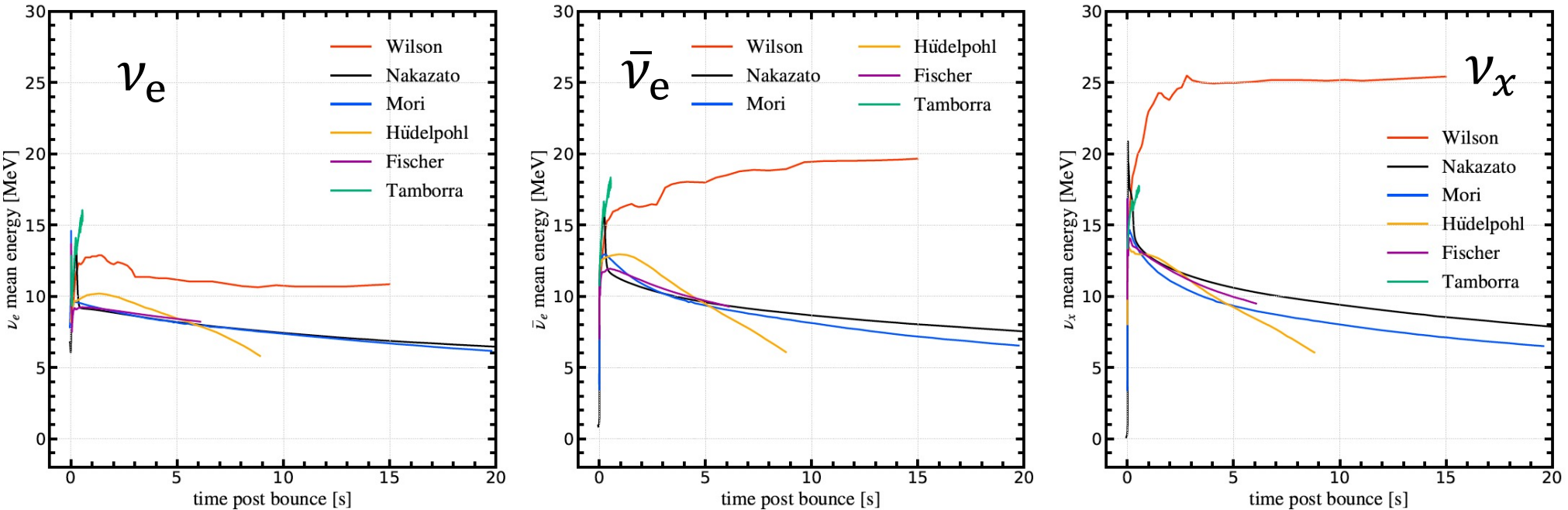


6 models
until 20s

Luminosity
vs. time



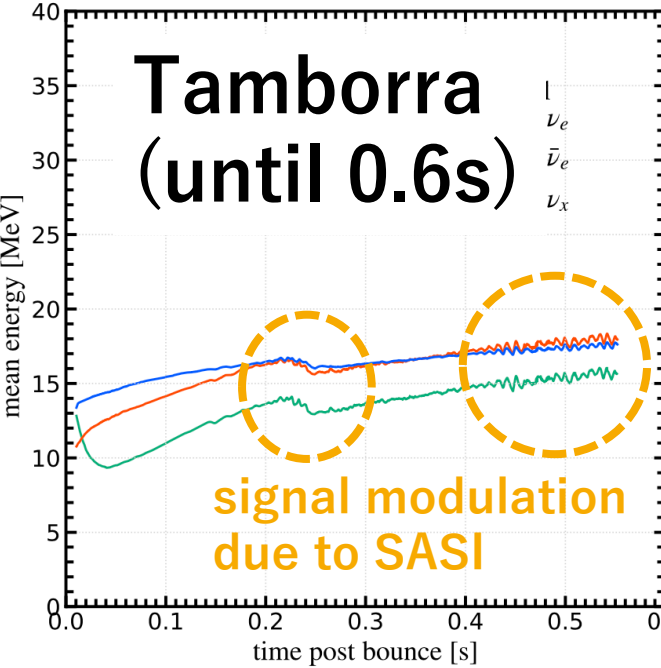
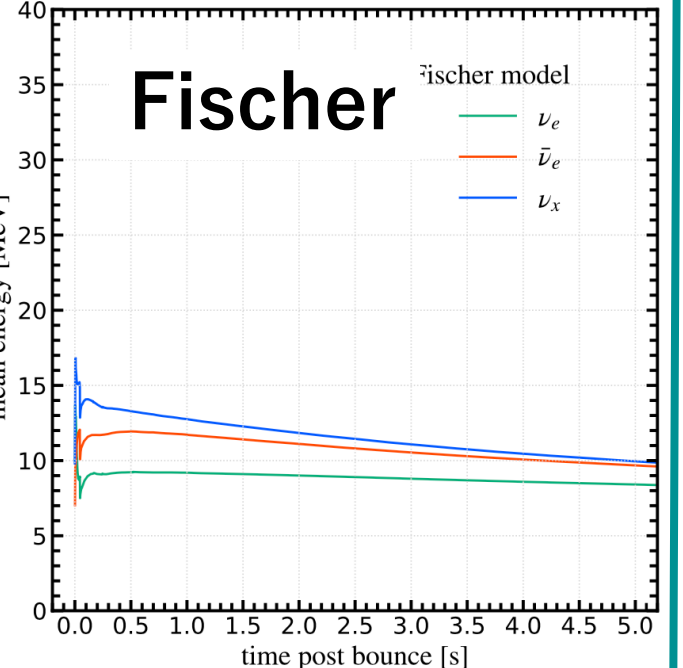
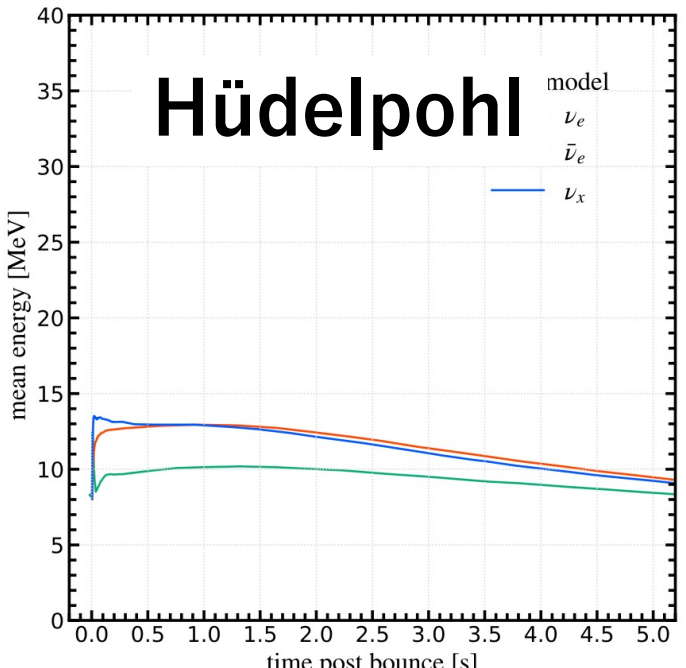
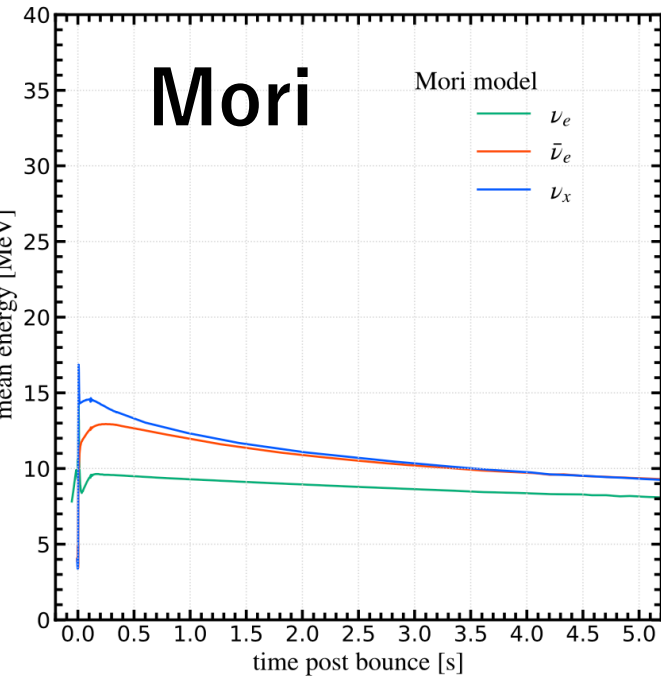
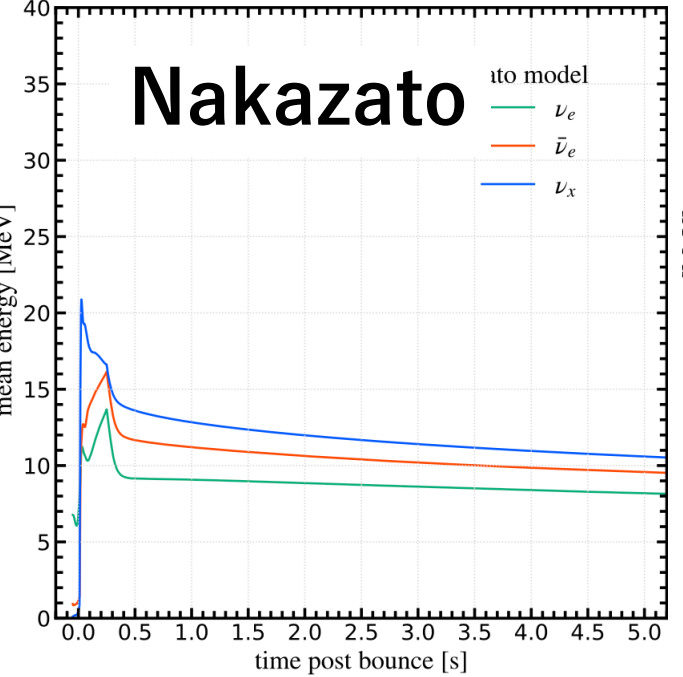
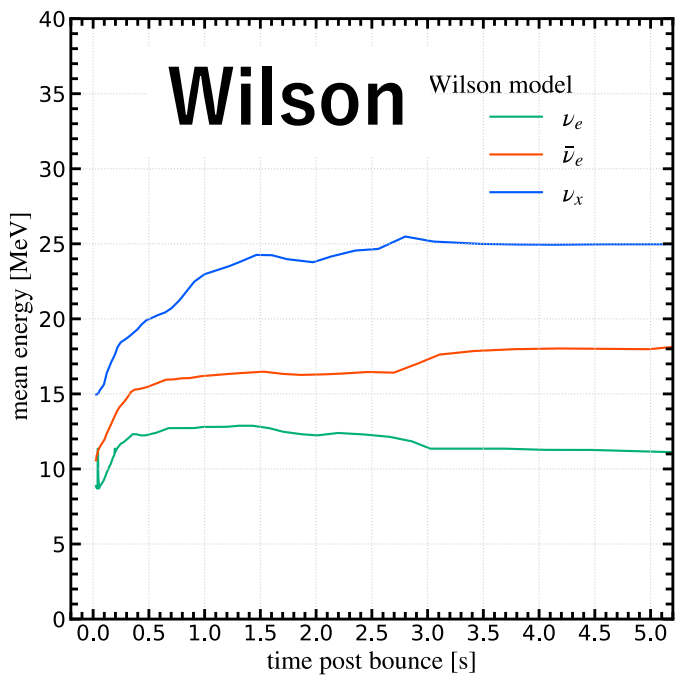
Mean energy
vs. time



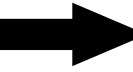
6 models
until 5s

Mean
energy
vs. time

ν_e
 $\bar{\nu}_e$
 ν_x



Data Format Unification

- “Nakazato format” 

Nakazato, K., et al. *ApJS* 205.1 (2013): 2
<http://asphwww.ph.noda.tus.ac.jp/snn/>

		$t_0 \leftarrow \text{time } t_n$					
E_0	E_1	$\frac{\Delta N_{1,\nu_e}(t_0)}{\Delta E_1}$	$\frac{\Delta N_{1,\bar{\nu}_e}(t_0)}{\Delta E_1}$	$\frac{\Delta N_{1,\nu_x}(t_0)}{\Delta E_1}$	$\frac{\Delta L_{1,\nu_e}(t_0)}{\Delta E_1}$	$\frac{\Delta L_{1,\bar{\nu}_e}(t_0)}{\Delta E_1}$	$\frac{\Delta L_{1,\nu_x}(t_0)}{\Delta E_1}$
E_1	E_2	$\frac{\Delta N_{2,\nu_e}(t_0)}{\Delta E_2}$	$\frac{\Delta N_{2,\bar{\nu}_e}(t_0)}{\Delta E_2}$	$\frac{\Delta N_{2,\nu_x}(t_0)}{\Delta E_2}$	$\frac{\Delta L_{2,\nu_e}(t_0)}{\Delta E_2}$	$\frac{\Delta L_{2,\bar{\nu}_e}(t_0)}{\Delta E_2}$	$\frac{\Delta L_{2,\nu_x}(t_0)}{\Delta E_2}$
energy		differential ν number flux			$\Delta N_{k,\nu_i}(t_n)/\Delta E_k$ [s ⁻¹ · MeV ⁻¹]		
\ddot{E}_k		$\frac{\Delta N_{20,\nu_e}(t_0)}{\Delta E_{20}}$	$\frac{\Delta N_{20,\bar{\nu}_e}(t_0)}{\Delta E_{20}}$	$\frac{\Delta N_{20,\nu_x}(t_0)}{\Delta E_{20}}$	$\frac{\Delta L_{20,\nu_e}(t_0)}{\Delta E_{20}}$	$\frac{\Delta L_{20,\bar{\nu}_e}(t_0)}{\Delta E_{20}}$	$\frac{\Delta L_{20,\nu_x}(t_0)}{\Delta E_{20}}$
E_{19}	E_{20}						

- Converting non-“Nakazato format” data to “Nakazato format”
 - time-integrated SN ν flux [MeV⁻¹ · kpc⁻²]

$$\frac{dF(E_\nu)}{dE_\nu} = \frac{1}{4\pi d_{\text{SN}}^2} \frac{E_{\nu_i,\text{total}}}{\langle E_{\nu_i} \rangle} f(E_\nu)$$

- ignore the distance term
 • replace $E_{\nu_i,\text{total}}$ [MeV] with $L_{\nu_i}(t)$ [erg · s⁻¹]
 • assume **Fermi-Dirac distribution** as $f(E_\nu)$

$$\frac{d^2N_\nu}{dE_\nu dt} = \frac{L_{\nu_i}(t)}{\langle E_{\nu_i} \rangle(t)} \frac{2}{3\zeta(3)T_{\nu_i}^3} \frac{E_\nu^2}{e^{E_\nu/T_{\nu_i}} + 1}$$

$L_{\nu_i}(t)$ and $\langle E_{\nu_i} \rangle(t)$ are usually available in every model

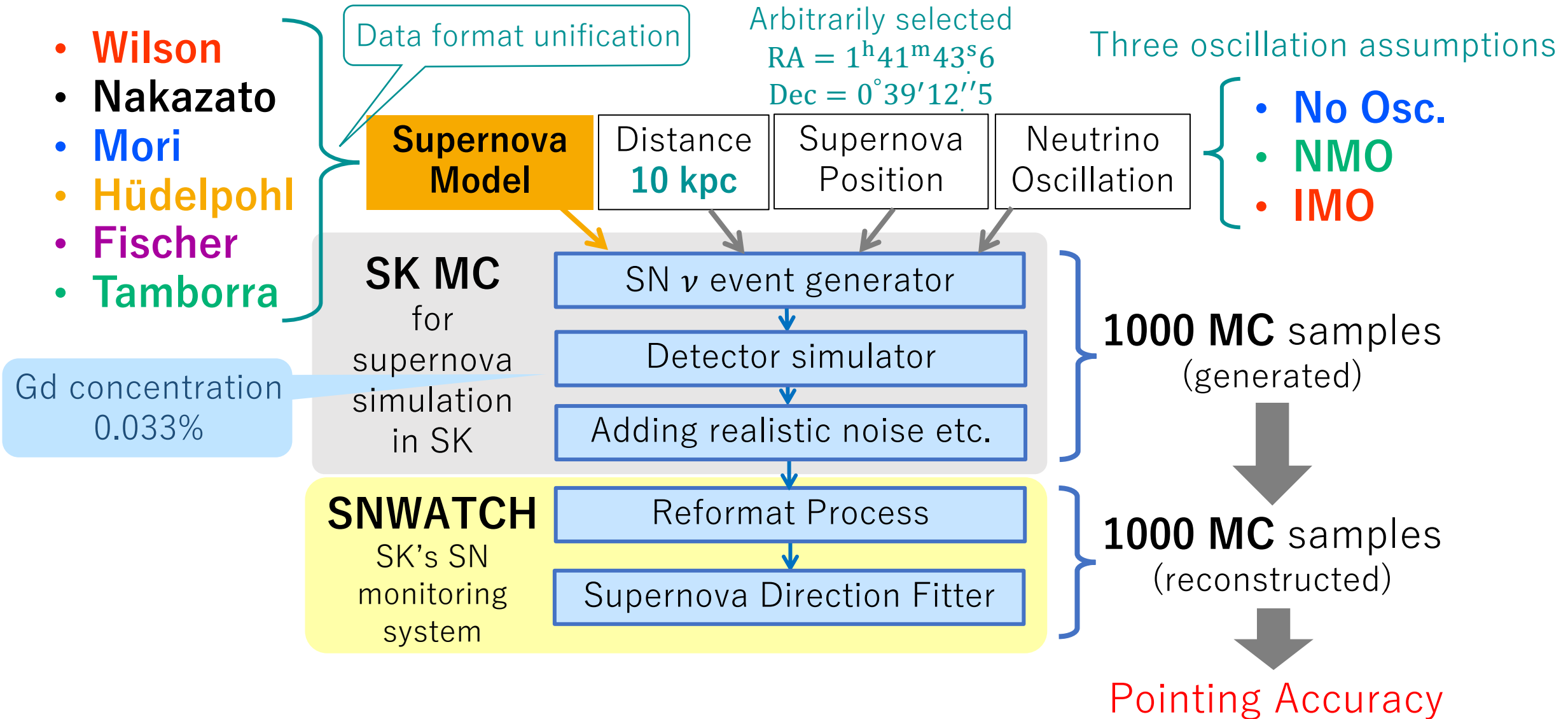
d_{SN} : distance to the supernova [kpc]
 $E_{\nu_i,\text{total}}$: total energy emitted by ν_i [MeV]
 $\langle E_{\nu_i} \rangle$: average energy of ν_i [MeV]
 $f(E_\nu)$: normalized distribution function

$$f_{\text{FD}}(E_\nu) = \frac{2}{3\zeta(3)T_{\nu_i}^3} \frac{E_\nu^2}{e^{E_\nu/T_{\nu_i}} + 1} \quad T_{\nu_i} = \frac{180}{7\pi^4} \zeta(3) \langle E_{\nu_i} \rangle \approx \frac{\langle E_{\nu_i} \rangle}{3.151}$$

$$\zeta(3) \approx 1.202$$

$$\frac{\Delta L_{k,\nu_i}(t_n)}{\Delta E_k} = \frac{\Delta N_{k,\nu_i}(t_n)}{\Delta E_k} \times E_k \times \frac{1.6022 \times 10^{-6} \text{ erg}}{\text{MeV}}$$

Detector Response and Pointing Accuracy for SN at 10 kpc



Average # of events generated by SKSNSim (32.5k m³)

Generated by	Wilson			Nakazato			Mori		
	SKSNSim	No Osc.	NMO	IMO	No Osc.	NMO	IMO	No Osc.	NMO
IBD ($\bar{\nu}_e$)	7431	8207	9970	3542	3893	4693	3275	3422	3745
ES (ν_e)	223	231	229	173	172	171	177	148	156
ES ($\bar{\nu}_e$)	97	97	98	63	66	72	60	61	63
ES (ν_x)	80	79	80	60	60	60	52	57	56
ES ($\bar{\nu}_x$)	69	69	69	52	51	48	45	45	44
total	8622	10530	12294	4074	4580	5389	3690	3904	4239

Generated by	Hüdelpohl			Fischer			Tamborra		
	SKSNSim	No Osc.	NMO	IMO	No Osc.	NMO	IMO	No Osc.	NMO
IBD ($\bar{\nu}_e$)	3048	3052	3049	1884	1990	2242	3830	3487	2718
ES (ν_e)	146	124	132	90	87	88	135	82	99
ES ($\bar{\nu}_e$)	53	53	53	35	35	37	50	45	35
ES (ν_x)	43	47	46	31	31	31	28	38	35
ES ($\bar{\nu}_x$)	38	38	38	27	26	25	25	26	30
total	3390	3398	3396	2100	2228	2487	4280	3919	3135

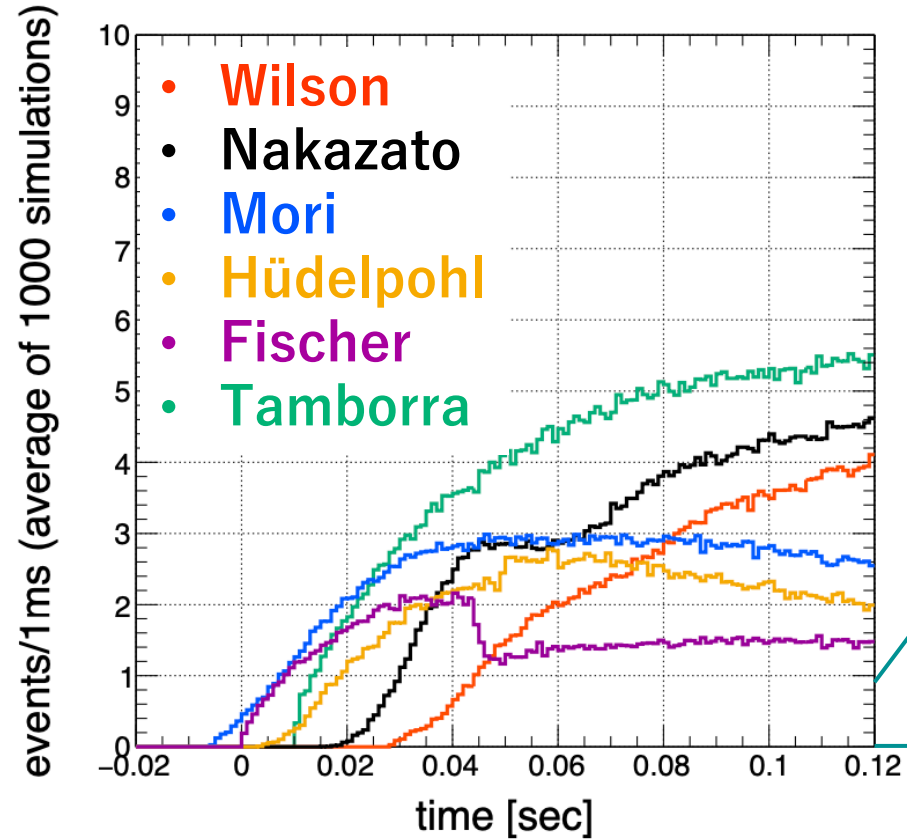
Average # of reconstructed events (22.5k m³)

Reconstructed	Wilson			Nakazato			Mori		
	No Osc.	NMO	IMO	No Osc.	NMO	IMO	No Osc.	NMO	IMO
IBD ($\bar{\nu}_e$)	4879	5364	6465	2221	2434	2921	2048	2144	2355
ES (ν_e)	69	106	95	43	57	53	44	46	45
ES ($\bar{\nu}_e$)	22	25	30	10	11	13	9	9	10
ES (ν_x)	34	28	30	18	16	17	15	14	14
ES ($\bar{\nu}_x$)	28	27	26	15	14	13	12	11	11
total	5185	6418	7505	2364	2681	3169	2151	2307	2520

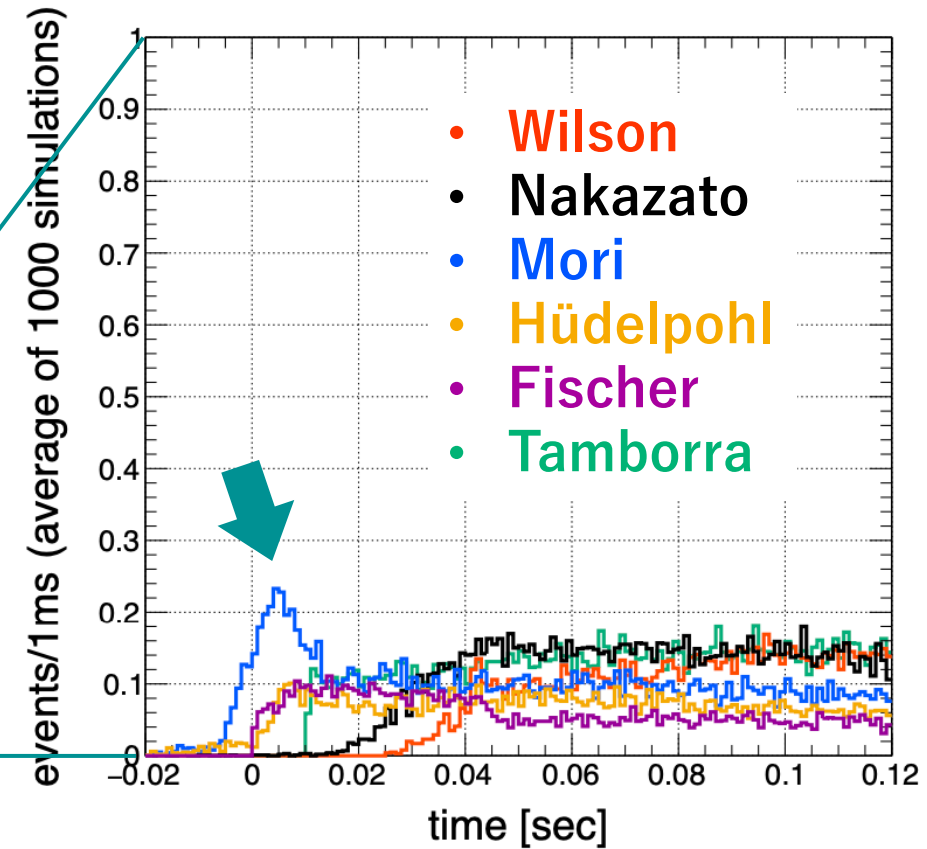
Reconstructed	Hüdelpohl			Fischer			Tamborra		
	No Osc.	NMO	IMO	No Osc.	NMO	IMO	No Osc.	NMO	IMO
IBD ($\bar{\nu}_e$)	1936	1939	1935	1186	1260	1437	2505	2283	1786
ES (ν_e)	38	39	39	22	29	26	46	33	37
ES ($\bar{\nu}_e$)	9	8	8	5	6	6	12	10	8
ES (ν_x)	12	12	12	9	8	8	10	12	12
ES ($\bar{\nu}_x$)	10	10	10	7	7	7	8	9	10
total	2031	2037	2041	1241	1338	1514	2678	2463	1953

Time Evolution until 0.12 s (SN@10kpc, NMO)

IBD



ES

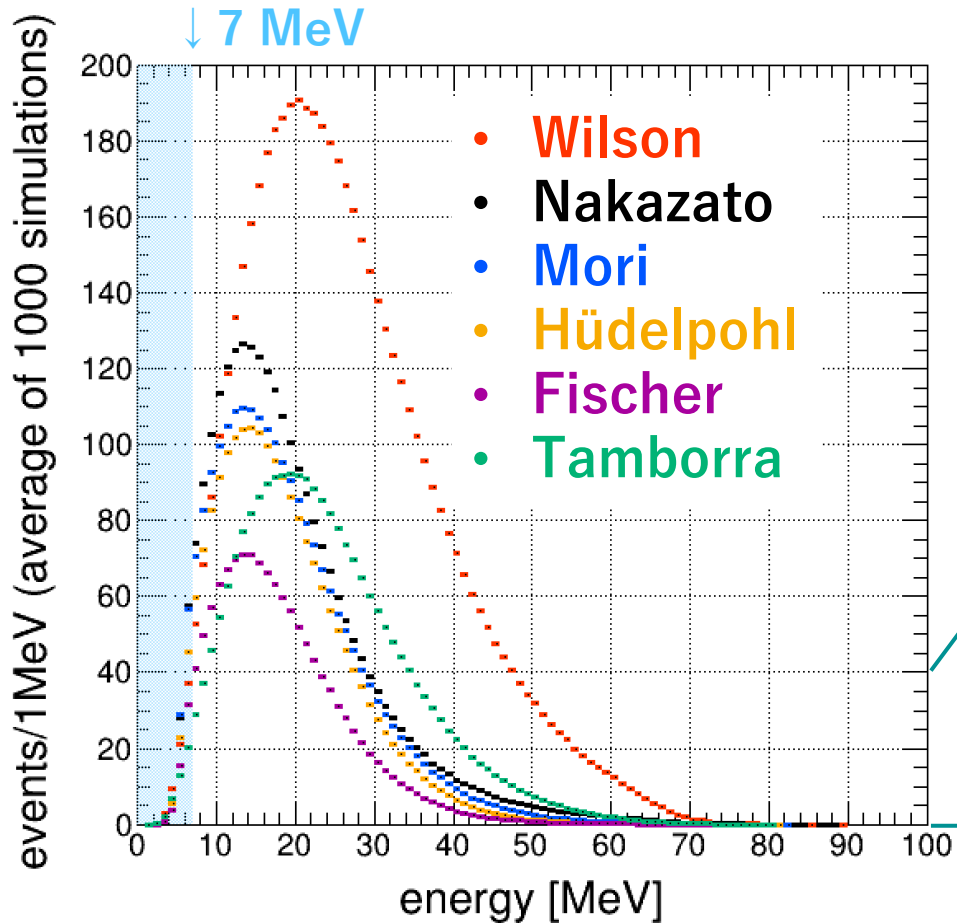


Difference in time structure can be used in model discrimination

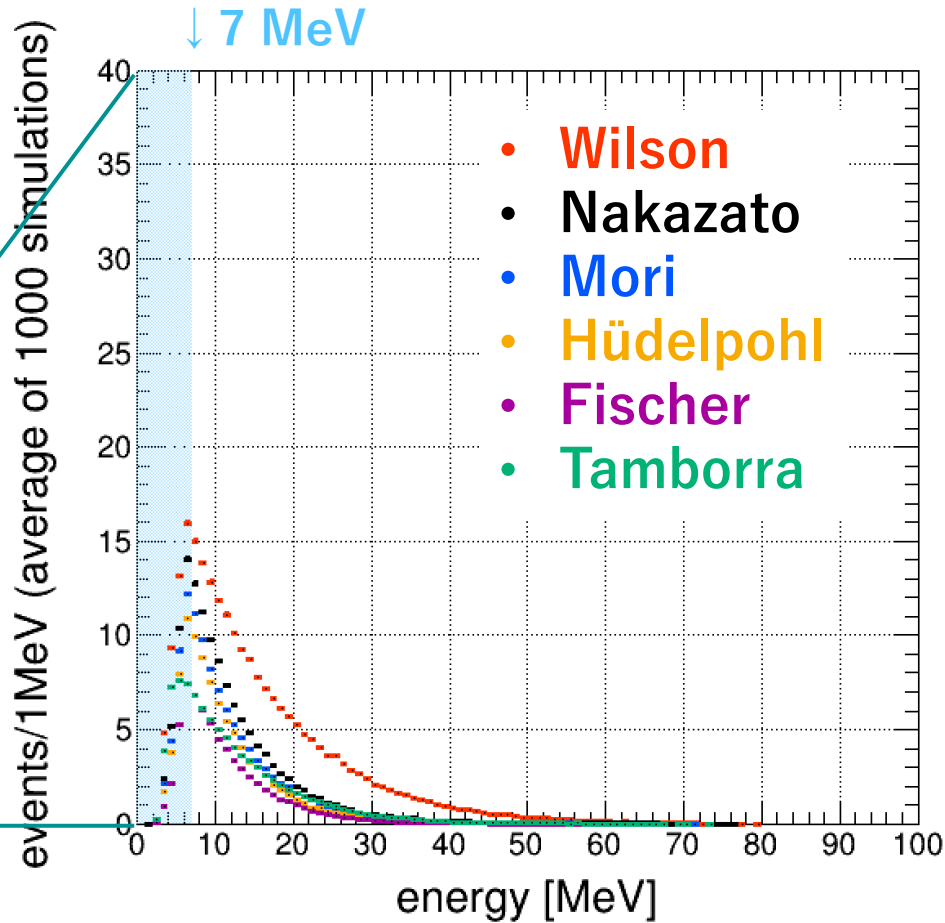
- Neutronization burst feature appeared as an ES event peak in Mori Model
 - possibly detectable for a closer SN

Reconstructed Energy (SN@10kpc, NMO)

IBD



ES

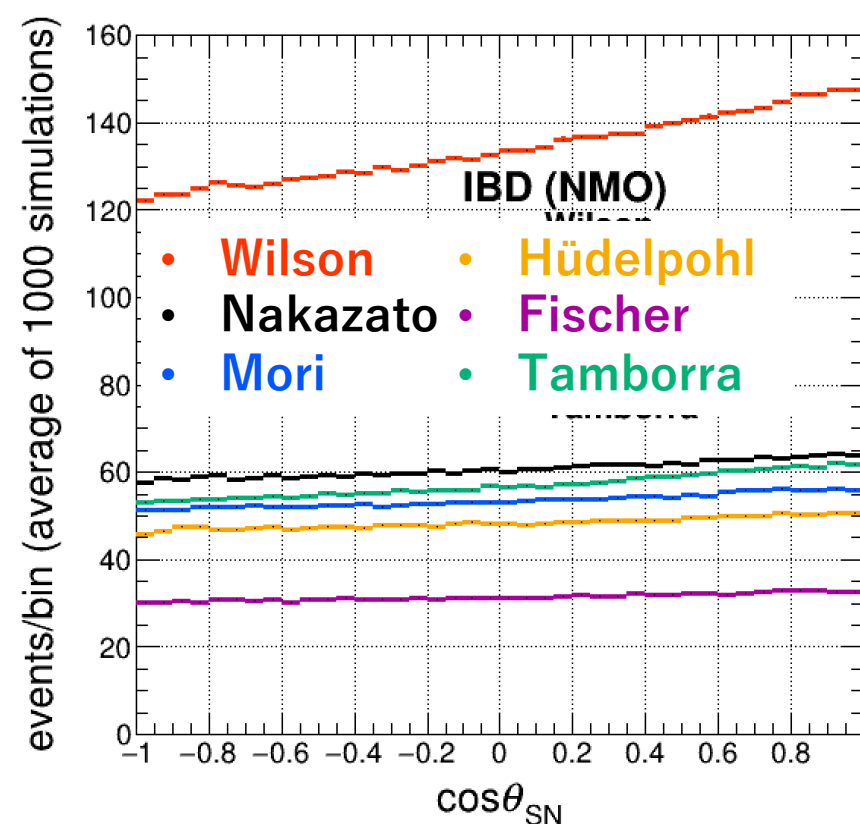


- Reconstructed e^+ energy
- Higher mean energy in **Wilson model** and **Tamborra model**

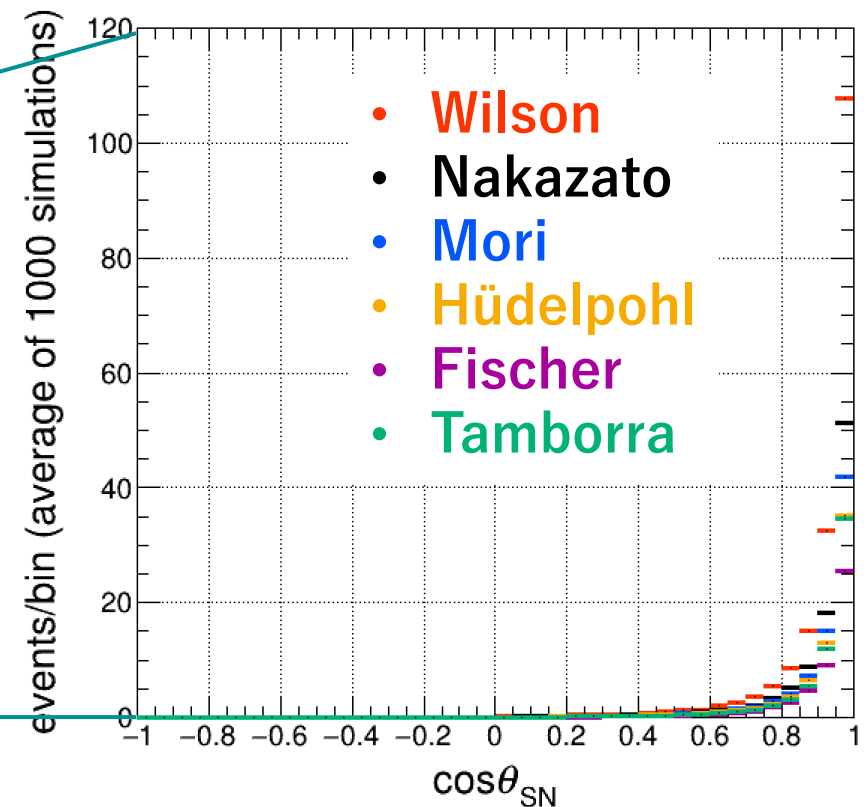
- Reconstructed e^- energy

Angular Distribution of Events: $\cos \theta_{\text{SN}}$ (SN@10kpc, NMO)

IBD

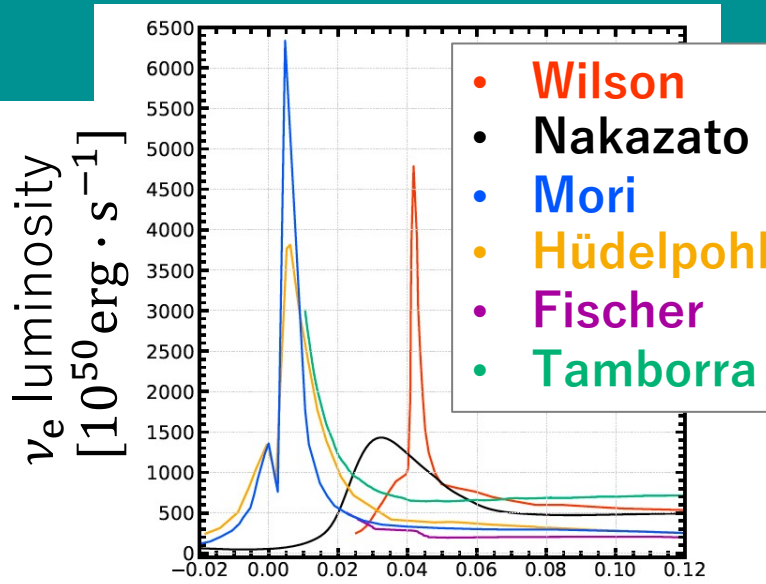


ES



- θ_{SN} : between true SN direction and e^+
- Almost flat distribution
- Forward inclination due to higher energy $\bar{\nu}_e$ (e^+)

- θ_{SN} : between true SN direction and e^-
- Peak at $\cos \theta_{\text{SN}} \sim 1$



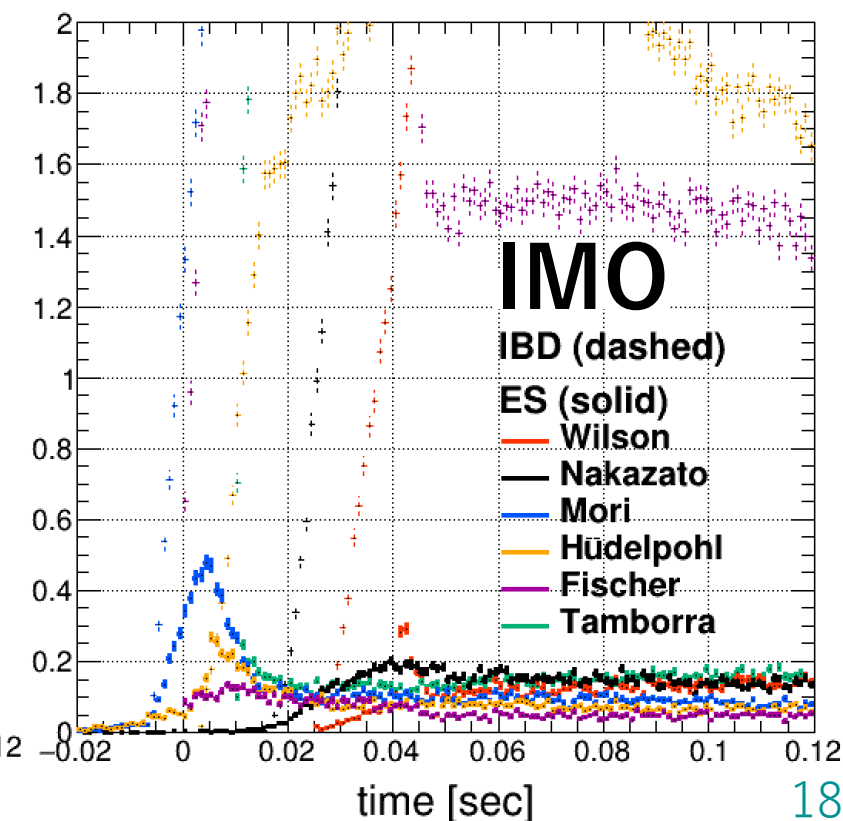
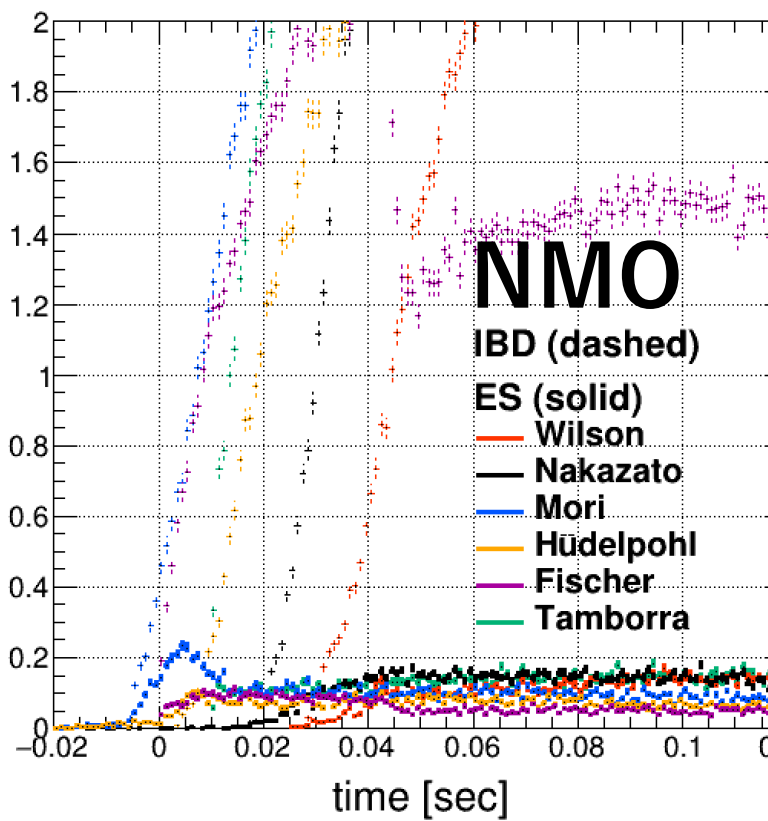
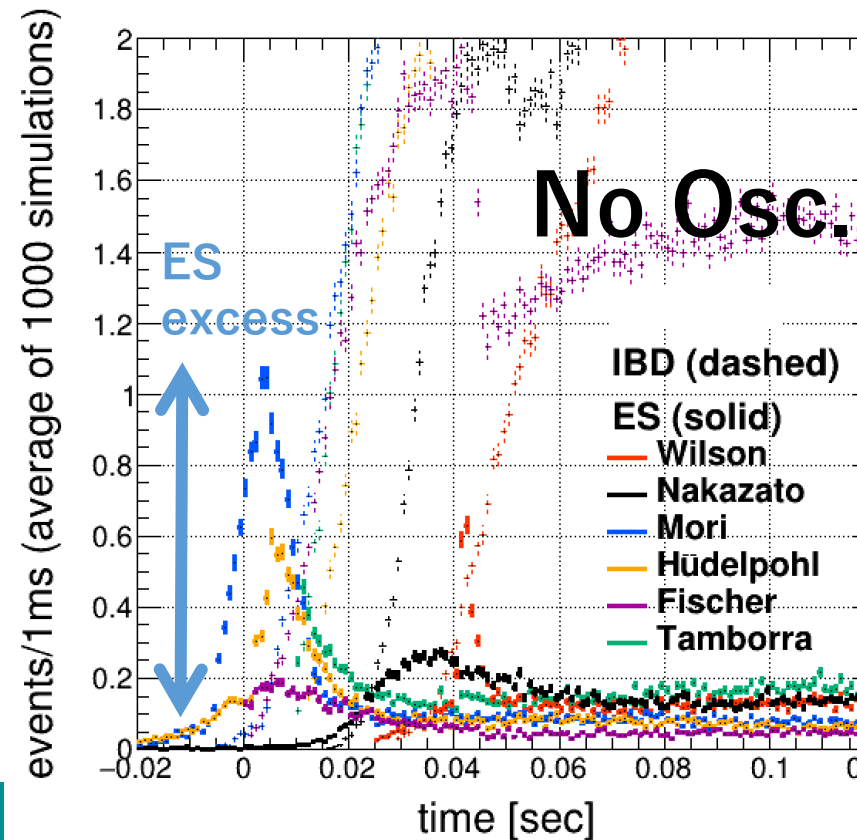
Result Detection of Neutronization Burst

- Appeared as an ES event peak

(Mori model) # of **ES events excess**
over flat components [events]

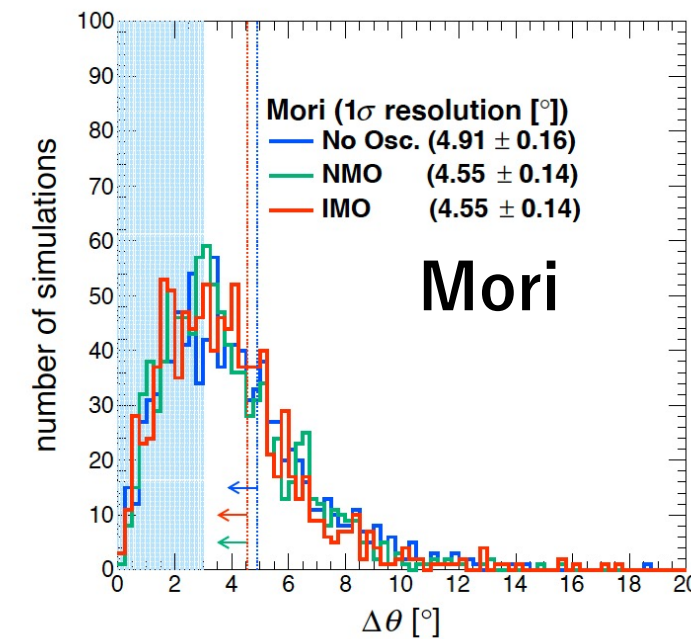
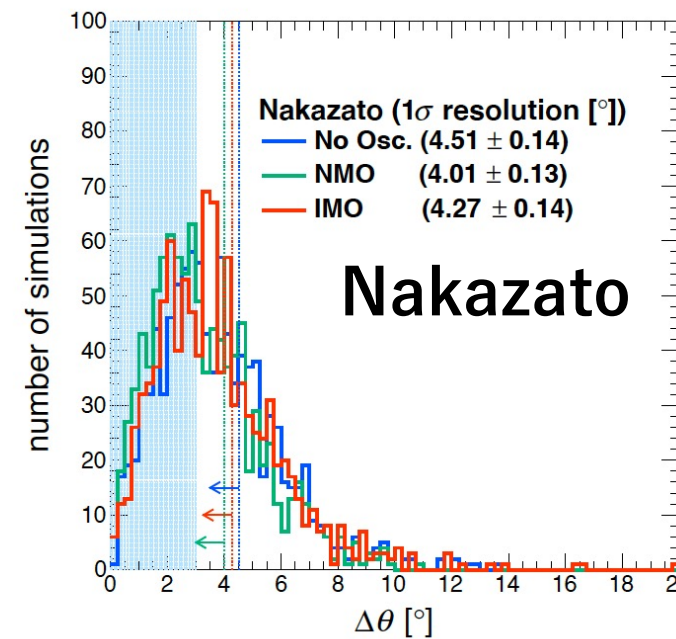
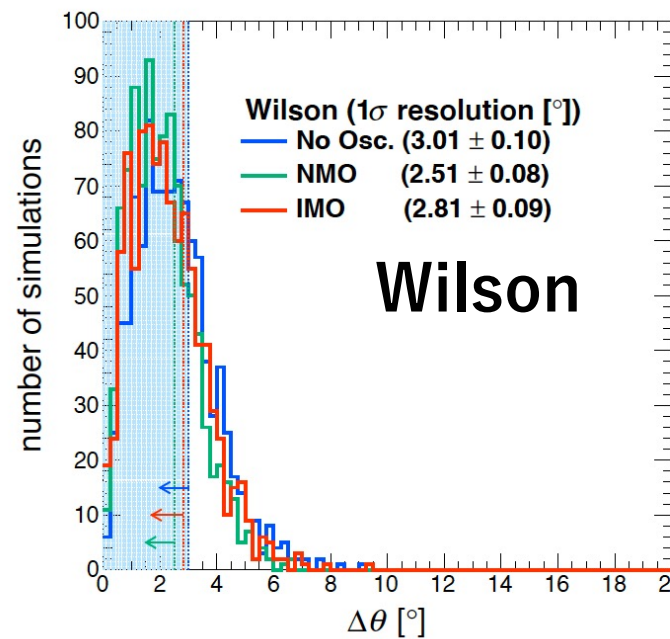
No Osc.	NMO	IMO
10.9 ± 0.10	1.32 ± 0.04	4.28 ± 0.07

→ A closer supernova
might enable SK's response
to distinguish NMO/IMO
using ES events peak

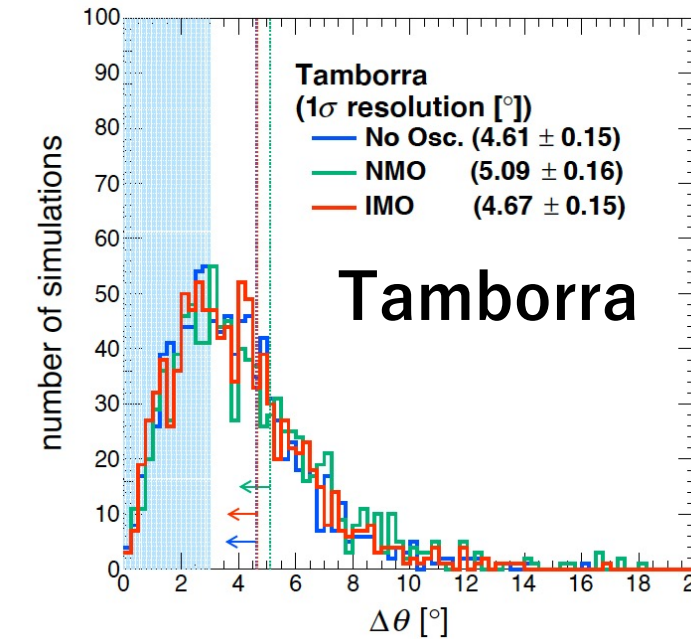
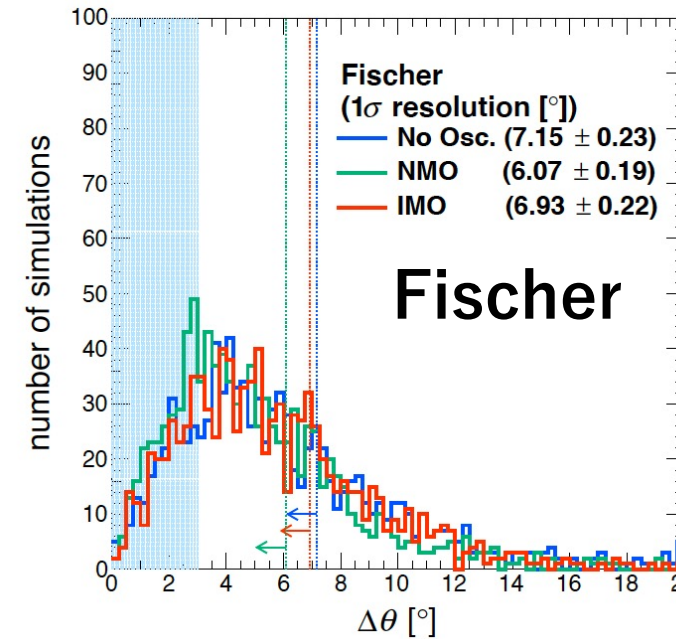
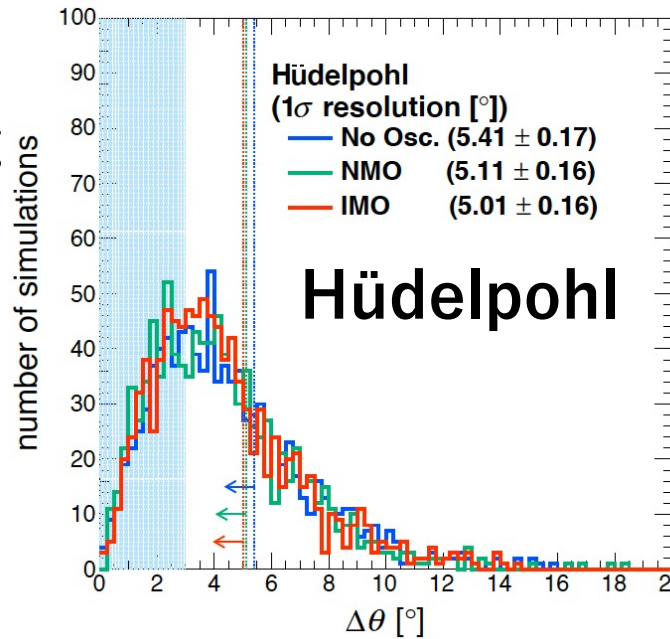


$\Delta\theta$ vs. # of MC

- SN@10kpc
- ν oscillation
 - No Osc.
 - NMO
 - IMO



- For determining pointing accuracy



Result Pointing Accuracy at 1σ [°]

ES/IBD Ratio

	Wilson	Nakazato								
Wilson	<table border="1"><tr><td>NMO</td><td>IMO</td></tr><tr><td>2.51±0.08</td><td>2.81±0.09</td></tr></table>	NMO	IMO	2.51±0.08	2.81±0.09	<table border="1"><tr><td>NMO</td><td>IMO</td></tr><tr><td>4.01±0.13</td><td>4.27±0.14</td></tr></table>	NMO	IMO	4.01±0.13	4.27±0.14
NMO	IMO									
2.51±0.08	2.81±0.09									
NMO	IMO									
4.01±0.13	4.27±0.14									
Mori	<table border="1"><tr><td>NMO</td><td>IMO</td></tr><tr><td>4.55±0.14</td><td>4.55±0.14</td></tr></table>	NMO	IMO	4.55±0.14	4.55±0.14	<table border="1"><tr><td>NMO</td><td>IMO</td></tr><tr><td>5.11±0.16</td><td>5.01±0.16</td></tr></table>	NMO	IMO	5.11±0.16	5.01±0.16
NMO	IMO									
4.55±0.14	4.55±0.14									
NMO	IMO									
5.11±0.16	5.01±0.16									
Fischer	<table border="1"><tr><td>NMO</td><td>IMO</td></tr><tr><td>6.07±0.19</td><td>6.93±0.22</td></tr></table>	NMO	IMO	6.07±0.19	6.93±0.22	<table border="1"><tr><td>NMO</td><td>IMO</td></tr><tr><td>5.09±0.16</td><td>4.67±0.15</td></tr></table>	NMO	IMO	5.09±0.16	4.67±0.15
NMO	IMO									
6.07±0.19	6.93±0.22									
NMO	IMO									
5.09±0.16	4.67±0.15									
Wilson	<table border="1"><tr><td>NMO</td><td>IMO</td></tr><tr><td>0.035±0.003</td><td>0.028±0.002</td></tr></table>	NMO	IMO	0.035±0.003	0.028±0.002	<table border="1"><tr><td>NMO</td><td>IMO</td></tr><tr><td>0.040±0.004</td><td>0.033±0.003</td></tr></table>	NMO	IMO	0.040±0.004	0.033±0.003
NMO	IMO									
0.035±0.003	0.028±0.002									
NMO	IMO									
0.040±0.004	0.033±0.003									
Mori	<table border="1"><tr><td>NMO</td><td>IMO</td></tr><tr><td>0.037±0.004</td><td>0.034±0.004</td></tr></table>	NMO	IMO	0.037±0.004	0.034±0.004	<table border="1"><tr><td>NMO</td><td>IMO</td></tr><tr><td>0.036±0.004</td><td>0.036±0.004</td></tr></table>	NMO	IMO	0.036±0.004	0.036±0.004
NMO	IMO									
0.037±0.004	0.034±0.004									
NMO	IMO									
0.036±0.004	0.036±0.004									
Fischer	<table border="1"><tr><td>NMO</td><td>IMO</td></tr><tr><td>0.040±0.006</td><td>0.033±0.005</td></tr></table>	NMO	IMO	0.040±0.006	0.033±0.005	<table border="1"><tr><td>NMO</td><td>IMO</td></tr><tr><td>0.028±0.004</td><td>0.038±0.005</td></tr></table>	NMO	IMO	0.028±0.004	0.038±0.005
NMO	IMO									
0.040±0.006	0.033±0.005									
NMO	IMO									
0.028±0.004	0.038±0.005									
Tamborra										

- For SN at 10 kpc:
 $3\text{--}7^\circ$
- 3° accuracy is achieved in Wilson model (SK-Gd's goal)
- Better pointing accuracy with Higher ES/IBD ratio.

◆ Summary

- First systematic study on SK's response and pointing accuracy since SK-Gd
- SK's responses to SN at 10kpc are simulated using six SN models by data format unification
 - SK's response varies in models, reflecting the t, E structure difference among models
 - indicating that SN model discrimination using SK's response is possible
- Pointing accuracy for SN at 10kpc varies in 3-7°
 - Wilson model achieves 3° accuracy (SK-Gd's goal)
 - Other models do not achieve it due to small statistics → need efforts to improve S/N ratio

◆ Prospects

- Quantitative discrimination of SN models using SK's response
- Exploring SK's response with more variety of SN models
- Improvements in pointing accuracy
 - by modifying the event reconstruction/neutron tagging algorithm.
- Can SK-Gd discriminate these SN candidates' explosion?

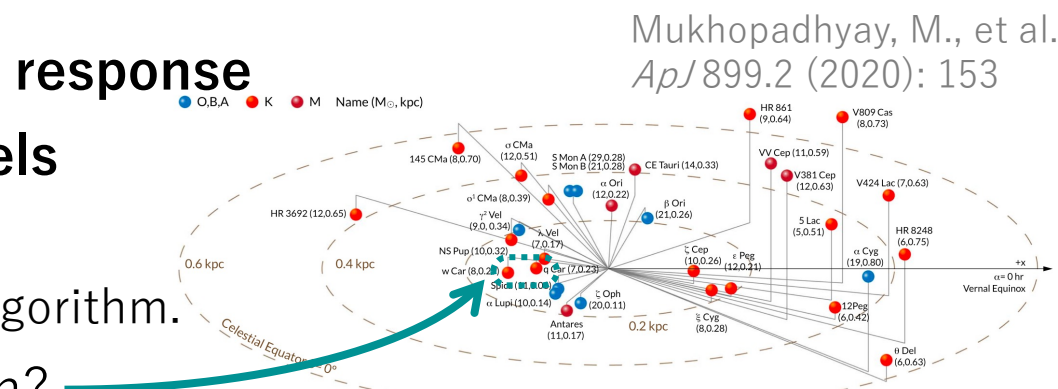


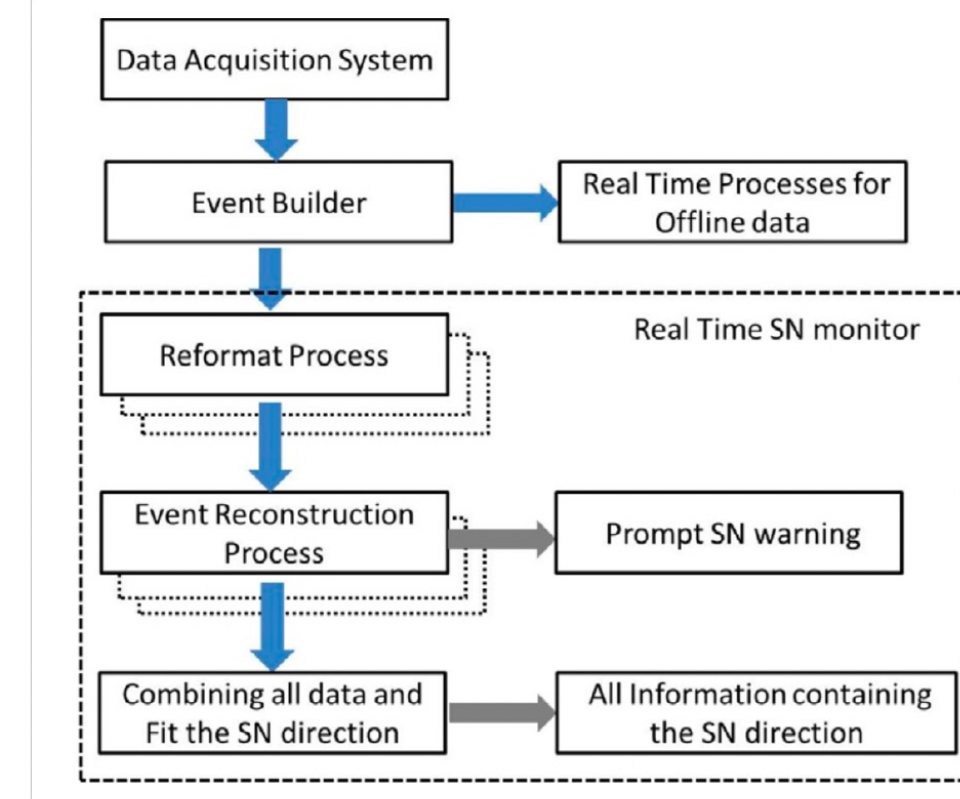
Figure 2. Illustration of nearby ($D \leq 1$ kpc) core collapse supernova candidates. Each star's spectral type, name, mass, and distance is shown in labels. See Table A1 for details and references.

Back up (2023/3/3)

SNWATCH: real-time supernova monitoring system @ SK

- Event reconstruction
 - Event vertex reconstruction
 - Event direction reconstruction
 - Event energy reconstruction
- Determination of SN direction
 - Dividing events into prompt/delayed candidates
 - Neutron tagging to flag IBD events
 - Maximum Likelihood Fit
- Alert Issue
 - SNWATCH aims to release the alert within less than ~1 min from the ν burst detection in SK

[Next slide](#)

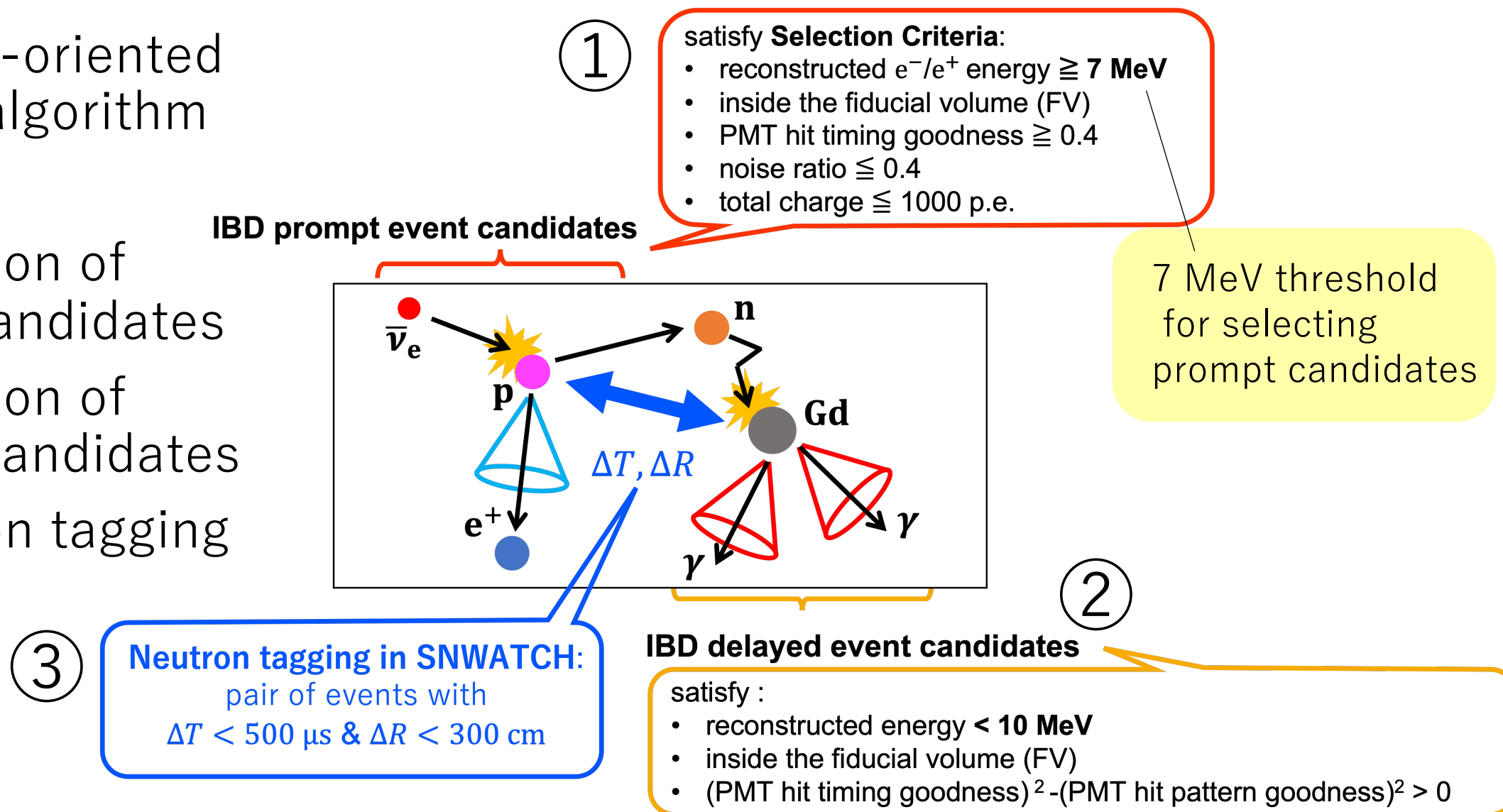


Block diagram of SNWATCH.

Event Selection and Neutron tagging in SNWATCH

- A speed-oriented simple algorithm

- ① Selection of prompt candidates
- ② Selection of delayed candidates
- ③ Neutron tagging



Determination of Supernova Direction in SNWATCH

- Maximum Likelihood Fit
 - Likelihood function for the i -th event

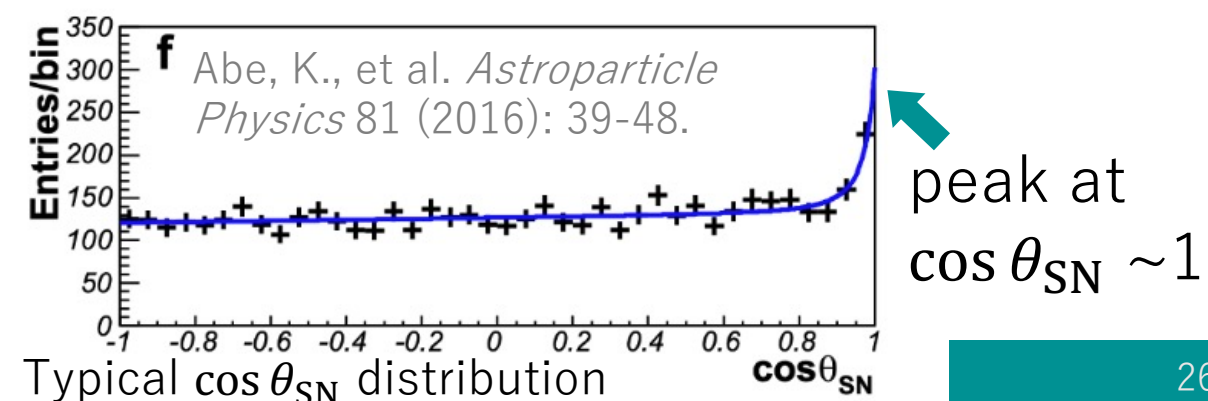
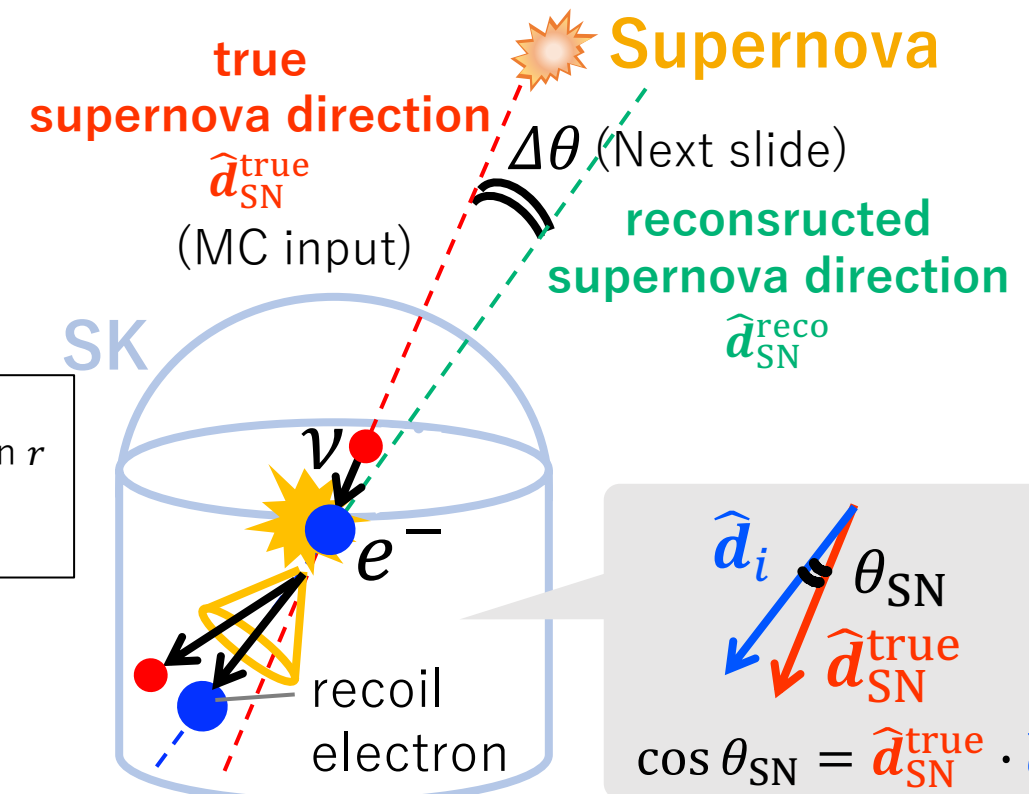
$$L_i = \sum_r N_{r,k} t_r(f_i) p_r(E_i, \hat{d}_i; \hat{d}_{SN}^{reco})$$

r : reaction (IBD, ES, oxygen CC), k : energy bin
 $N_{r,k}$: number of event k -th energy bin for reaction r
 $t_r(f_i)$: tagging efficiency term, E_i : energy
 $p(r)$: PDF function (determined by SK MC)

- Likelihood

$$\mathcal{L} = \exp \left\{ \sum_{k,r} N_{r,k} \right\} \prod_i L_i$$

- Maximized by $\frac{\partial \mathcal{L}}{\partial N_{r,k}} = \frac{\partial \mathcal{L}}{\partial \hat{d}_{SN}^{reco}} = 0$
- For ES, $\cos \theta_{SN}$ peaks at $\cos \theta_{SN} \sim 1$



Neutrino Oscillation in SKSNSim

- Matter effect for 3-flavor ν oscillation inside the supernova
 - $N_{\nu_i}^{gen}$: the # of ν_i ($i = e, x$, $x = \mu$ **or** τ) generated in a collapsing star
 - $N_{\nu_i}^{sur}$: the # of ν_i ($i = e, x$, $x = \mu$ **and** τ) at the stellar surface

Neutrino oscillation in NMO

Normal Mass Ordering: $m_1^2 < m_2^2 \ll m_3^2$

$$N_{\nu_e}^{sur} = N_{\nu_x}^{gen}$$

$$N_{\nu_x}^{sur} = N_{\nu_e}^{gen} + N_{\nu_x}^{gen}$$

$$N_{\bar{\nu}_e}^{sur} = N_{\bar{\nu}_e}^{gen} \times \cos^2 \theta_{12} + N_{\bar{\nu}_x}^{gen} \times \sin^2 \theta_{12}$$

$$N_{\bar{\nu}_x}^{sur} = N_{\bar{\nu}_e}^{gen} \times \sin^2 \theta_{12} + N_{\bar{\nu}_x}^{gen} \times (1 + \cos^2 \theta_{12})$$

Neutrino oscillation in IMO

Inverted Mass Ordering: $m_3^2 \ll m_1^2 < m_2^2$

$$N_{\nu_e}^{sur} = N_{\nu_e}^{gen} \times \sin^2 \theta_{12} + N_{\nu_x}^{gen} \times \cos^2 \theta_{12}$$

$$N_{\nu_x}^{sur} = N_{\nu_e}^{gen} \times \cos^2 \theta_{12} + N_{\nu_x}^{gen} \times (1 + \sin^2 \theta_{12})$$

$$N_{\bar{\nu}_e}^{sur} = N_{\bar{\nu}_x}^{gen}$$

$$N_{\bar{\nu}_x}^{sur} = N_{\bar{\nu}_e}^{gen} + N_{\bar{\nu}_x}^{gen}.$$

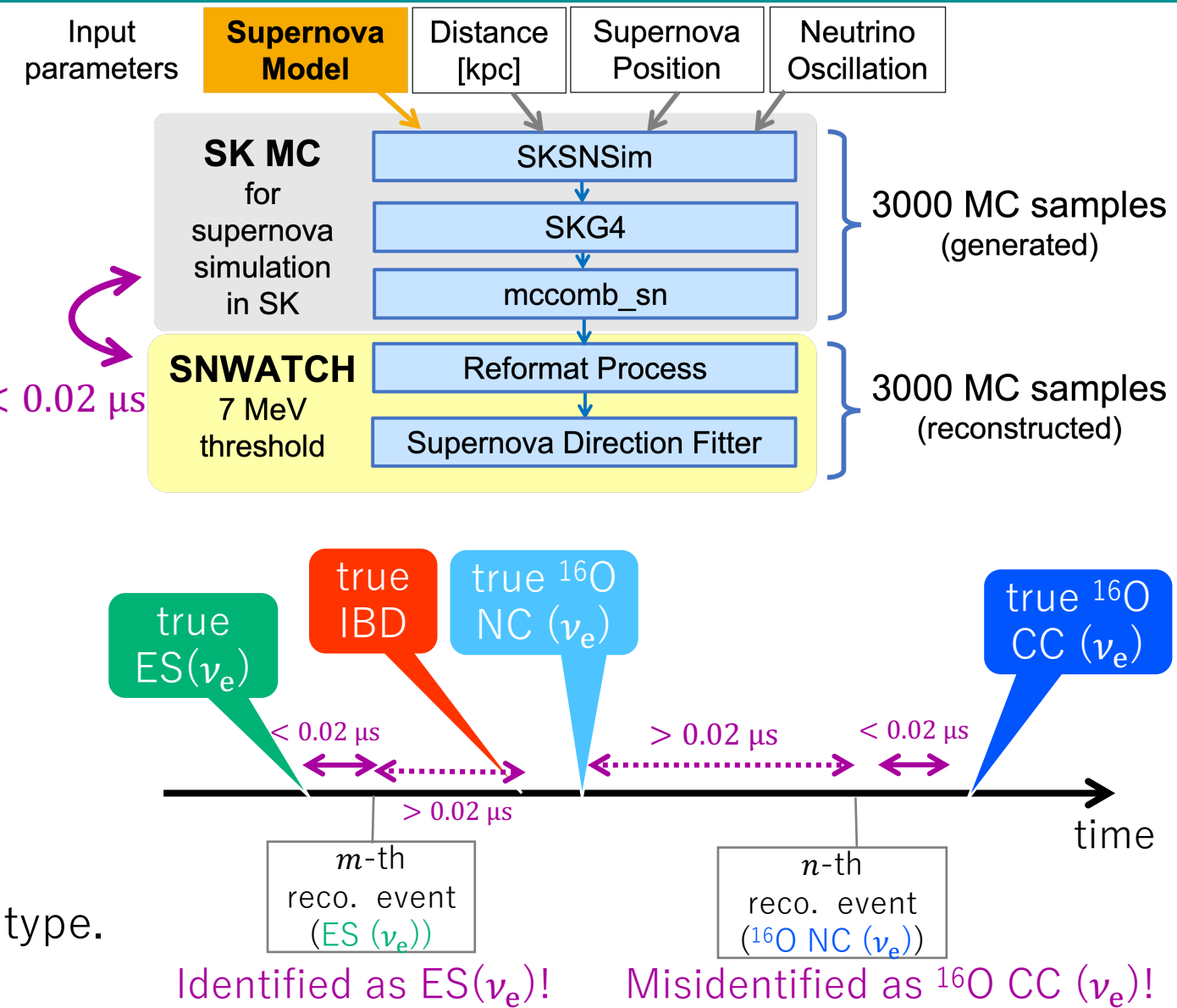
Oscillation parameter: $\sin^2 \theta_{12} = 0.307$ ($\cos^2 \theta_{12} = 0.693$)

Alert issue in SNWATCH

- Three types of alarm
 - **golden**: event cluster $>7\text{MeV}$, with uniform vertex distribution, cluster size ≥ 100
 - **normal**: event cluster $>7\text{MeV}$, with uniform vertex distribution, $25 \leq \text{cluster size} < 100$
 - **silent**: event cluster $>7\text{MeV}$, with uniform vertex distribution, cluster size < 25
- SNWATCH sends the golden alarm to:
 - SNEWS 1.0 (SuperNova Early Warning System 1.0)
P. Antonioli et al., New Journal of Physics 6 (2004) 114.
K. Scholberg, Astronomische Nachrichten: Astronomical Notes 329 (2008) 337–339.
 - IAU CBAT (International Astronomical Union Central Bureau for Astronomical Telegrams)
<http://www.cbat.eps.harvard.edu/>
 - ATEL (Astronomer's telegram) <http://www.astronomerstelegram.org/>
R. E. Rutledge, Publication of the Astronomical Society of the Pacific 110 (1998) 754.
 - GCN (The Gamma-ray Coordinates Network) <http://gcn.gsfc.nasa.gov>
S. D. Barthelmy et al., in AIP Conference Proceedings , vol. 526, pp. 731–735, American Institute of Physics. 2000
- False alarm rate
 - once in 9.0×10^7 years (=90 million years) for golden alarm
 - once in 4.7×10^5 years (=470 thousand years) for normal alarm

Difficulty in Performing Realistic SN simulation

- For realistic SN simulation, noise is added in `mccomb_sn`, resulting in a loss of original information generated in SKSNSim.
- To identify which type of interaction the reconstructed event was, $t_{\text{true}} - t_{\text{reco}} < 0.02 \mu\text{s}$ is used.
- Association = identification of interaction type
- Average association efficiency: 93% other than NC (Nakazato model)
- If the ν does not deposit enough energy, it is difficult to know the true interaction type.

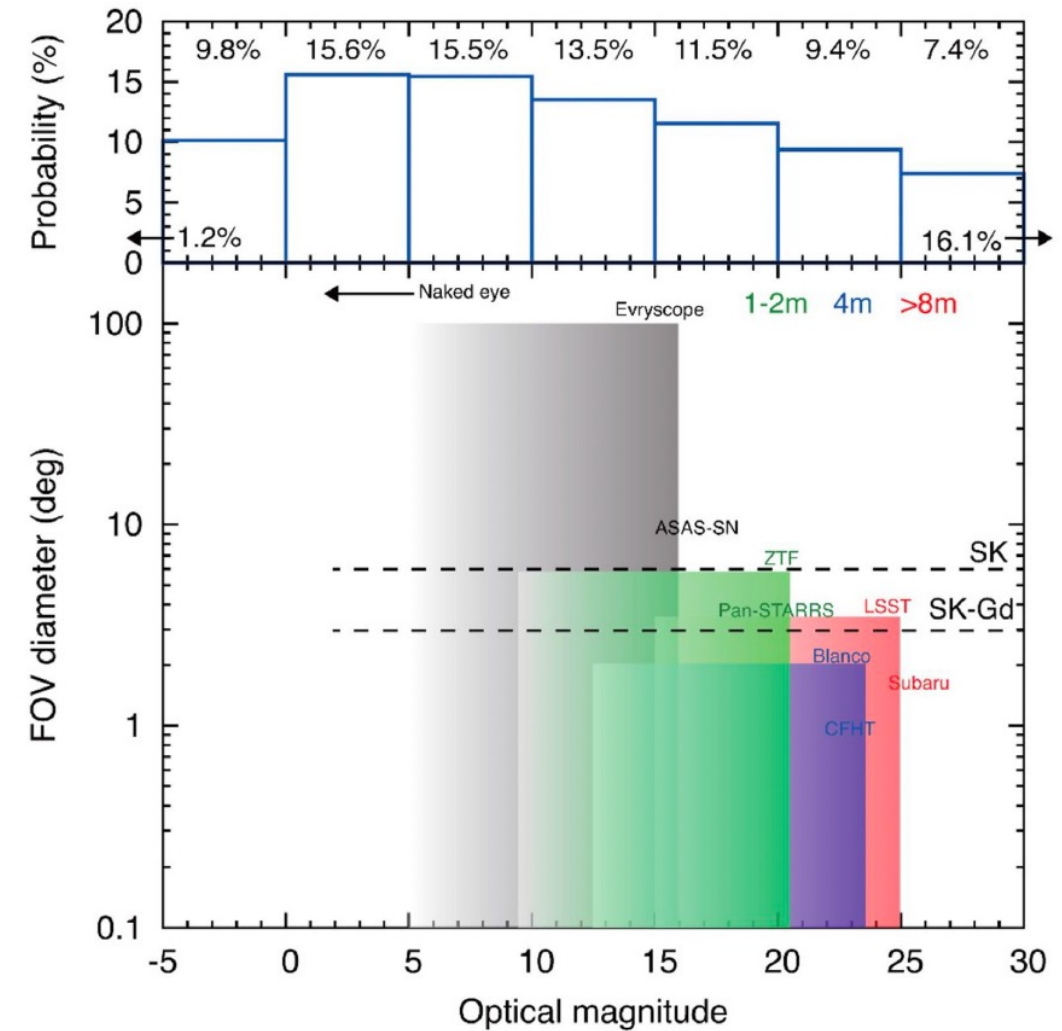


SN detection prospects

Nakamura, Ko, et al. *MNRAS* 461.3 (2016): 3296-3313.

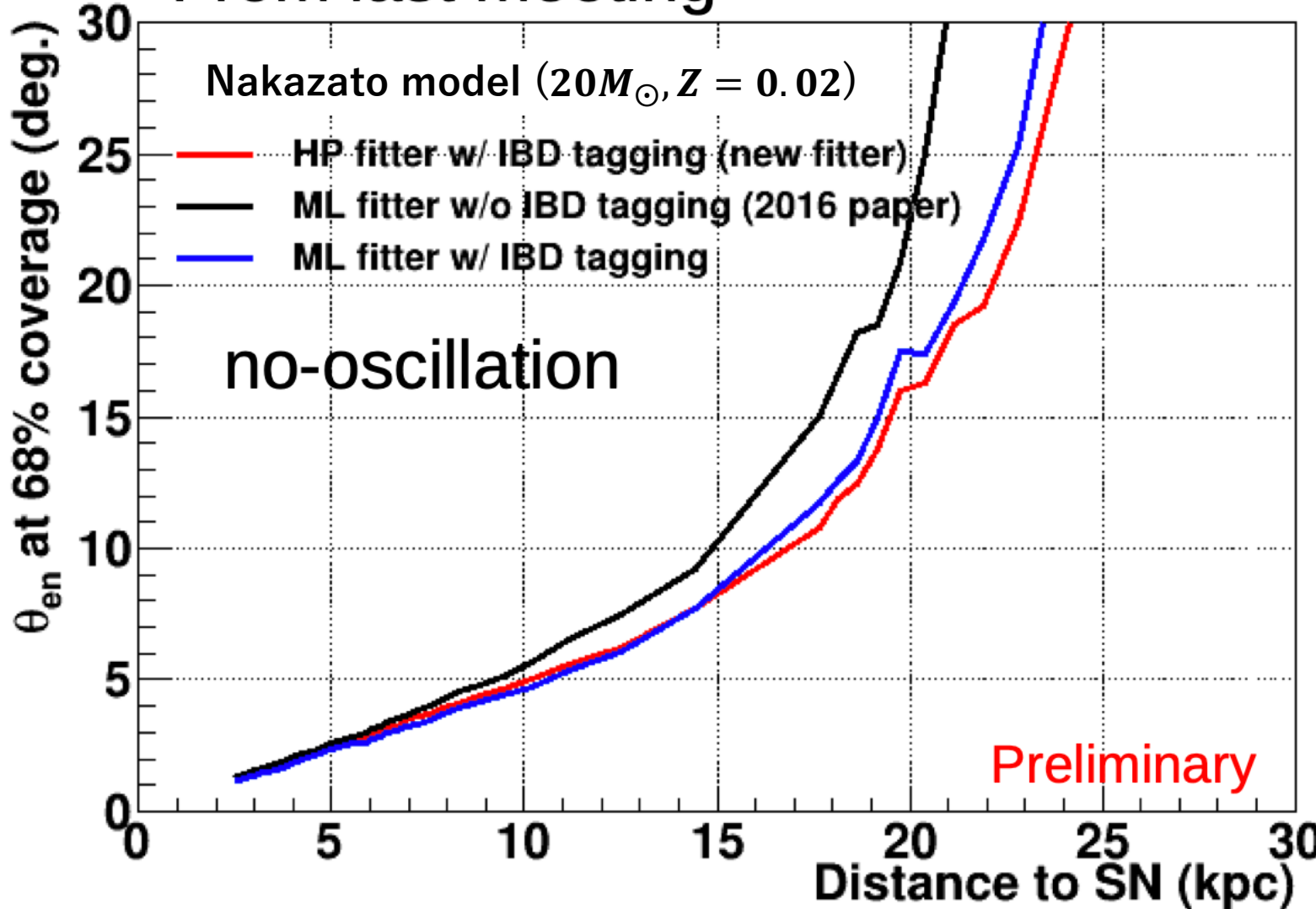
- SK-Gd has been aimed to determine SN direction with $\sim 3^\circ$ accuracy
- Large telescope's FOV (field of view)
 - e.g.,
 - Subaru(8.2 m in diameter)
Hyper Supreme-Cam: $\sim 1.5^\circ$
 - Vera C. Rubin Observatory
LSST (8.4 m in diameter): $\sim 3.5^\circ$

Fig. 2.22: Detection prospects of galactic supernovae [57]. (Top) The histograms of dust-attenuated plateau magnitudes of core-collapse supernovae and their respective percentage relative to the total core-collapse supernovae. (Bottom) The typical ranges of optical magnitude and fields of view (FOV) of various optical telescopes are shown by shaded rectangles: ASAS-SN (All-Sky Automated Survey for SuperNovae), Blanco, CFHT (Canada France Hawaii Telescope), Evryscope, LSST (Large Synoptic Survey Telescope), Pan-STARRS (Panoramic Survey Telescope and Rapid Response System), Subaru, and ZTF (Zwicky Transient Facility). The left-pointing arrow represents the optical magnitude sensitive to the naked eye. Pointing Accuracy of SK (pure water, $\sim 5^\circ$) and SK-Gd ($\sim 3^\circ$) are represented by the horizontal dashed lines and labeled.



SN Distance vs. Pointing Accuracy

From last meeting



ML fitter:
Maximum Likelihood Fitter

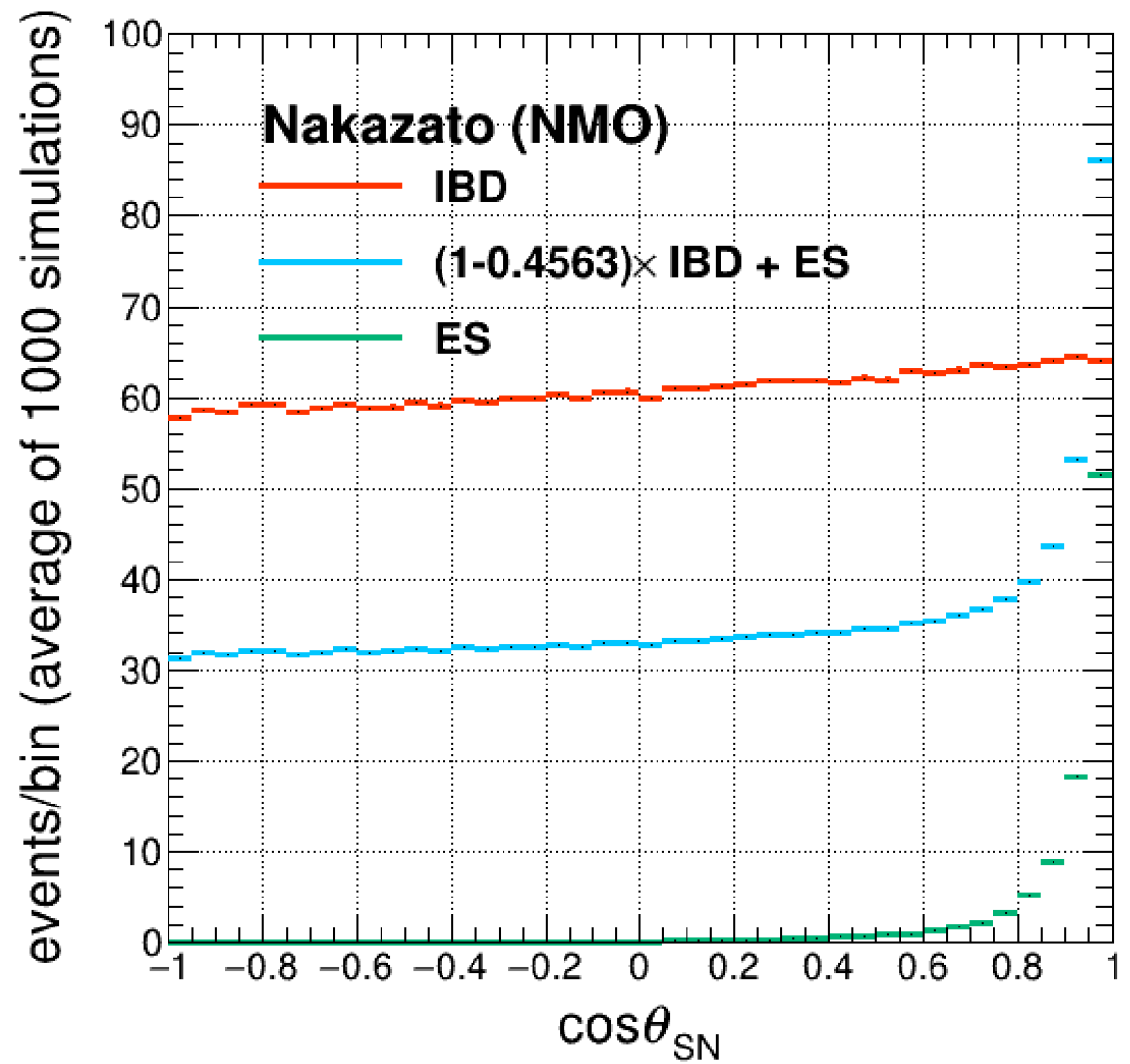
HP fitter:
HEALPix Fitter

made by
Guillaume-san
(SK Collaboration meeting
2022 Autumn)

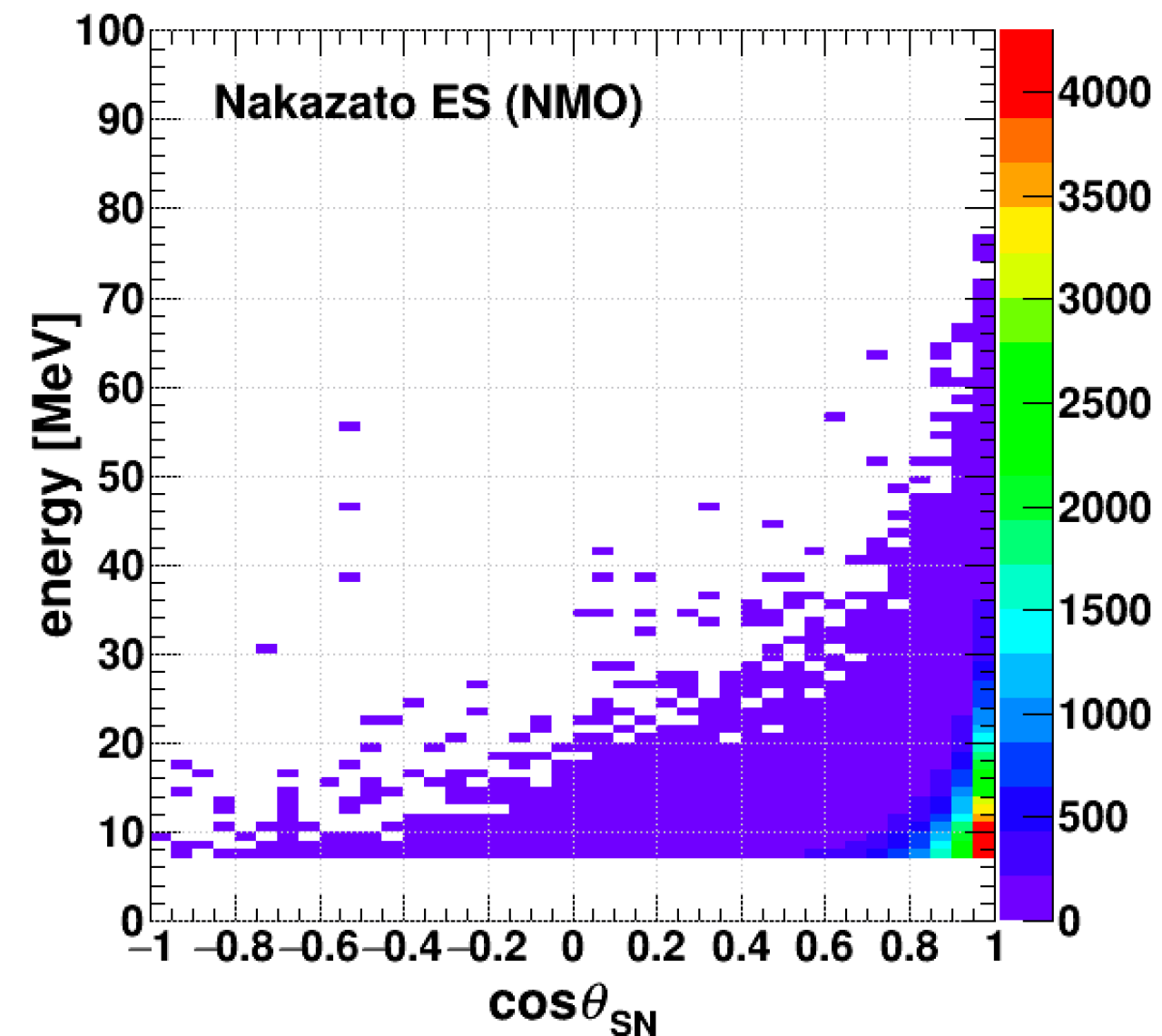
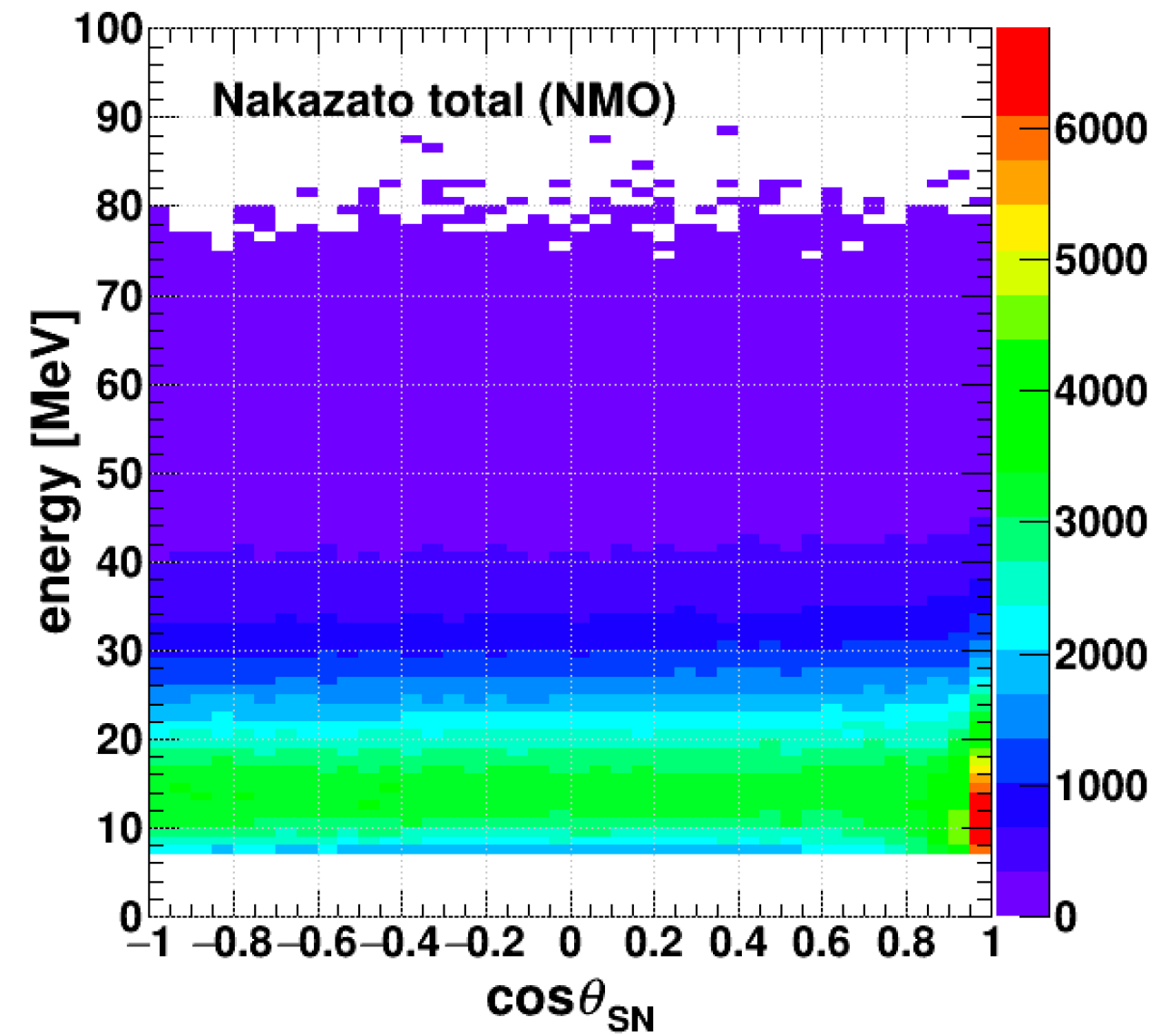
Results (Back up)

$\cos \theta_{\text{SN}}$ with tagging inefficiency (Nakazato SN@10kpc NMO)

- Neutron tagging efficiency in SNWATCH: 45.63%
- $(100-45.63)=54.37\%$ of IBD events are not flagged
→ worsening pointing accuracy
- Improvement of neutron tagging efficiency in SNWATCH is needed.



Reconstructed energy vs. $\cos \theta_{\text{SN}}$ (Nakazato SN@10kpc NMO)



Pointing Accuracy at 1σ (SN @10kpc)

Table 4.5: Pointing accuracy at 1σ in the unit of degree for six models with three oscillation cases. For each model, the gray column represents which of NMO and IMO provides better pointing accuracy.

	Wilson			Nakazato		
	No Osc.	NMO	IMO	No Osc.	NMO	IMO
Pointing accuracy [°]	3.01±0.10	2.51±0.08	2.81±0.09	4.51±0.14	4.01±0.13	4.27±0.14

	Mori			Hüdelpohl		
	No Osc.	NMO	IMO	No Osc.	NMO	IMO
Pointing accuracy [°]	4.91±0.16	4.55±0.14	4.55±0.14	5.41±0.17	5.11±0.16	5.01±0.16

	Fischer			Tamborra		
	No Osc.	NMO	IMO	No Osc.	NMO	IMO
Pointing accuracy [°]	7.15±0.23	6.07±0.19	6.93±0.22	4.61±0.15	5.09±0.16	4.67±0.15

Reconstructed ES/IBD event ratio (SN @10kpc)^{Satisfying}

- selection criteria
- $t_{\text{true}} - t_{\text{reco}} < 0.02 \mu\text{s}$

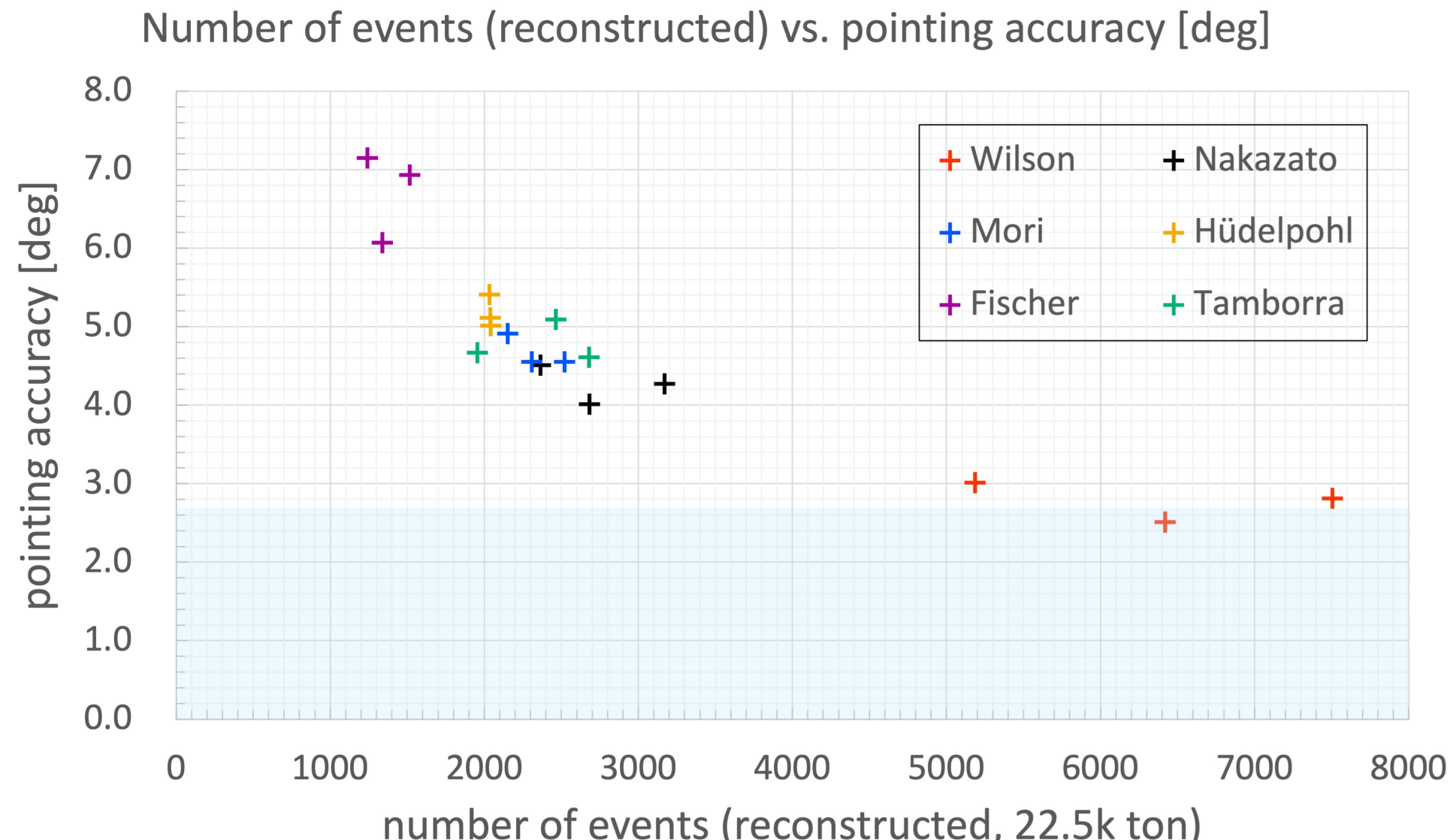
Table 4.6: The ratio of ES relative to IBD for six models with three oscillation cases. For each model, the gray column represents which of the NMO and IMO provides a higher ratio of ES/IBD.

	Wilson			Nakazato		
	No Osc.	NMO	IMO	No Osc.	NMO	IMO
ES/IBD	0.031±0.003	0.035±0.003	0.028±0.002	0.039±0.004	0.040±0.004	0.033±0.003

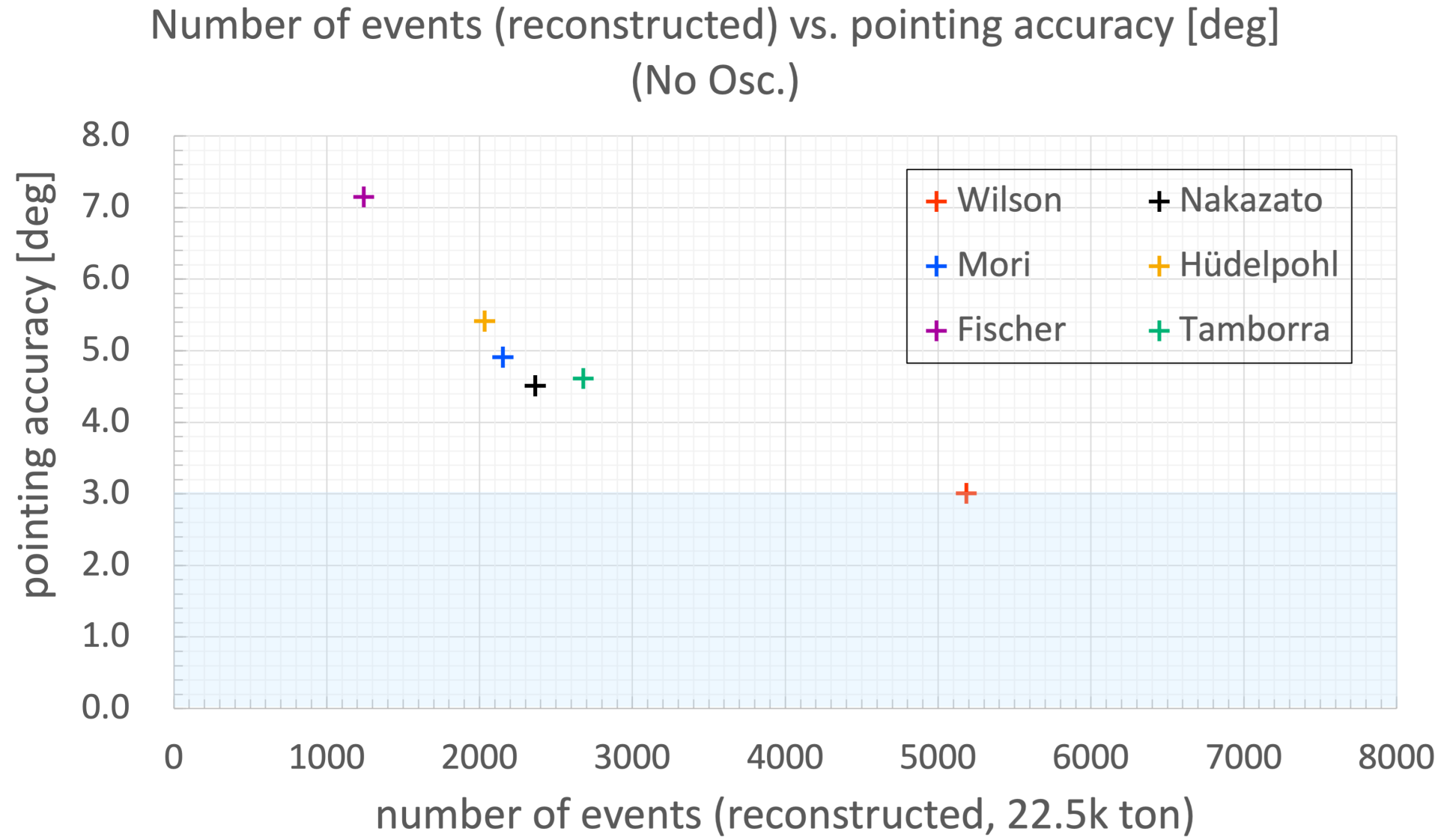
	Mori			Hüdelpohl		
	No Osc.	NMO	IMO	No Osc.	NMO	IMO
ES/IBD	0.039±0.004	0.037±0.004	0.034±0.004	0.036±0.004	0.036±0.004	0.036±0.004

	Fischer			Tamborra		
	No Osc.	NMO	IMO	No Osc.	NMO	IMO
ES/IBD	0.036±0.006	0.040±0.006	0.033±0.005	0.030±0.004	0.028±0.004	0.038±0.005

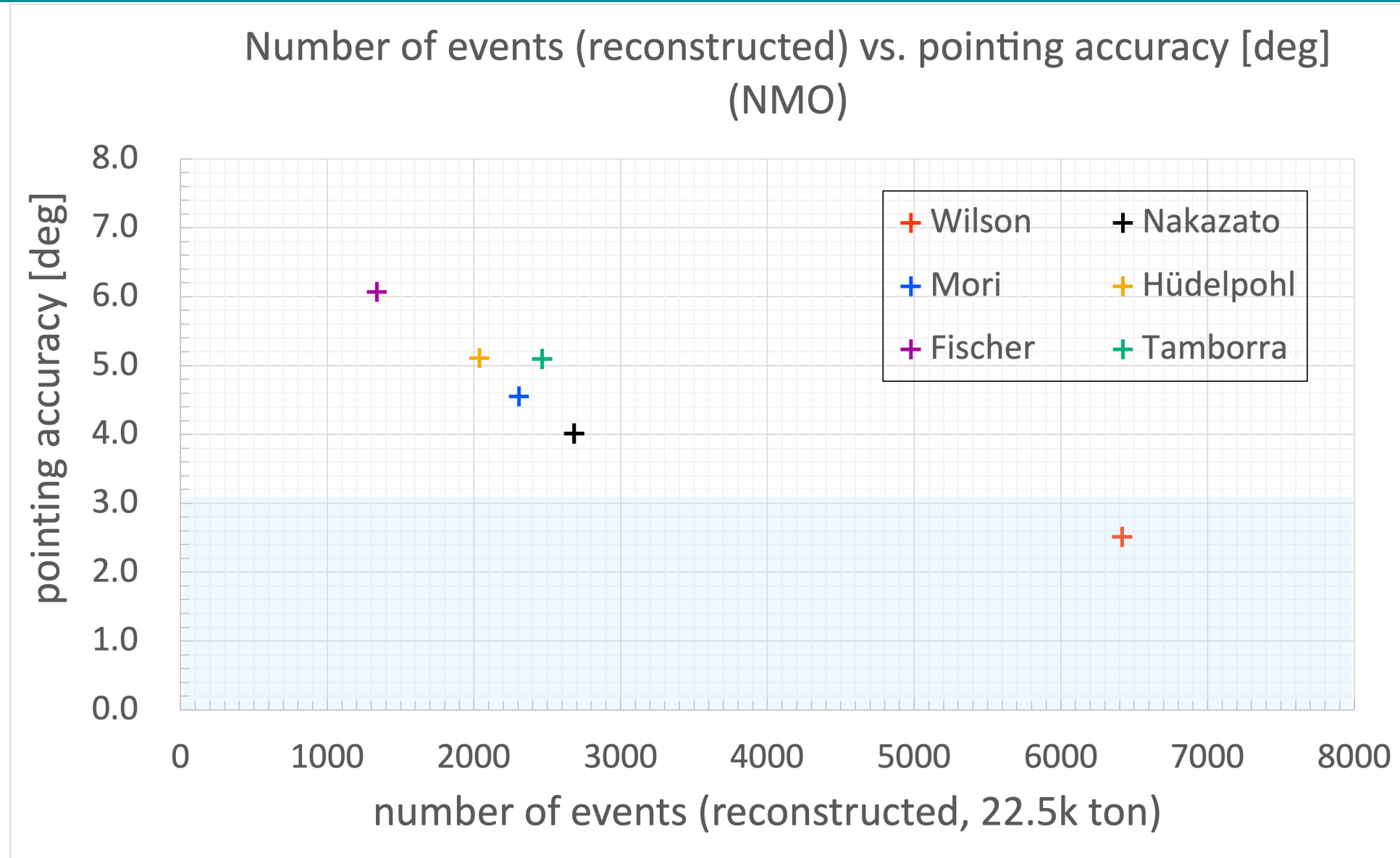
Observed events vs. Pointing Accuracy (10kpc, No Osc./NMO/IMO)



Observed events vs. Pointing Accuracy (10kpc, No Osc.)

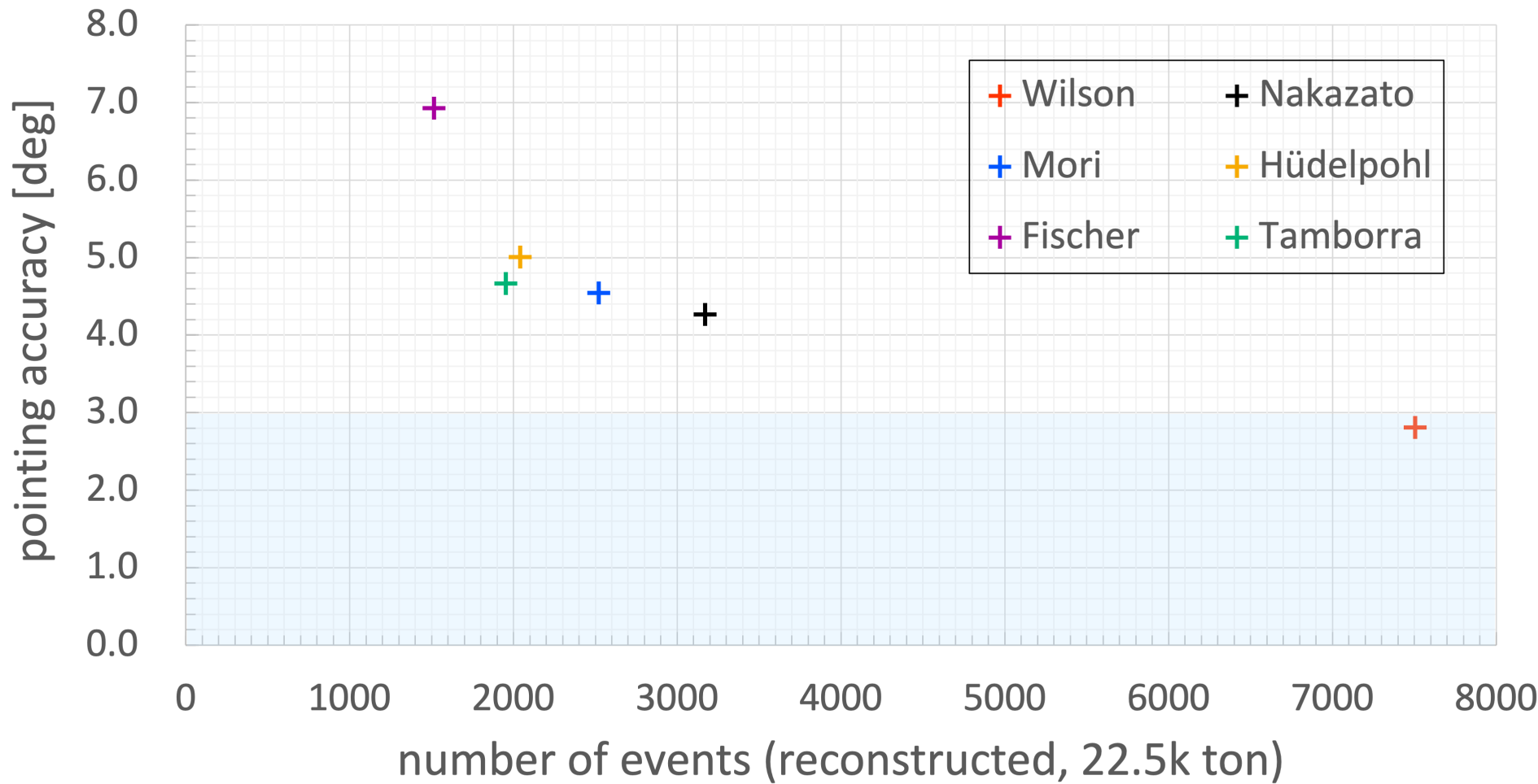


Observed events vs. Pointing Accuracy (10kpc, NMO)



Observed events vs. Pointing Accuracy (10kpc, IMO)

Number of events (reconstructed) vs. pointing accuracy [deg]
(IMO)



Prospects (Back up)

- SN model discrimination
- Identification of Nearby SN candidates

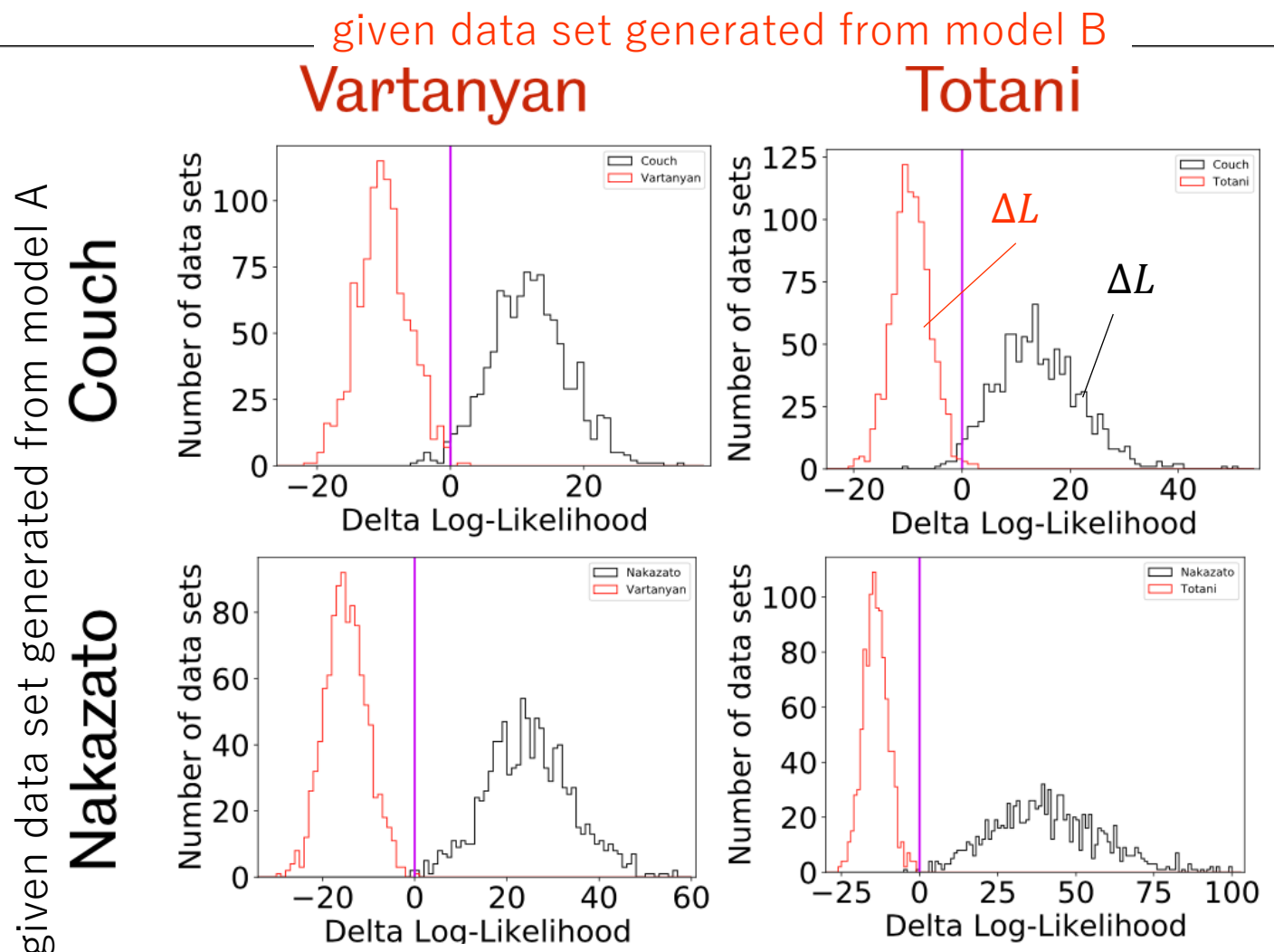
Model Discrimination using Likelihood

SN model discrimination with Hyper-K
Abe, K., et al. *ApJ* 916.1 (2021): 15.

- Employ the method of Abe, K., et al. *ApJ* 916.1 (2021): 15.
- Using simulated SN with a fixed # of total events
- Calculate the difference of log-likelihood for models A and B:

$$L = \sum_{i=1}^{N_{\text{obs}}} \ln \left(\sum_{\alpha} N_{i,\alpha} \right)$$

- i : (time, energy) bin index
- α : interaction channel index
- If $|\Delta L| > 5$, it is judged as a successful discrimination



Identification of Nearby SN candidates

Mukhopadhyay, M., et al. *ApJ* 899.2 (2020): 153

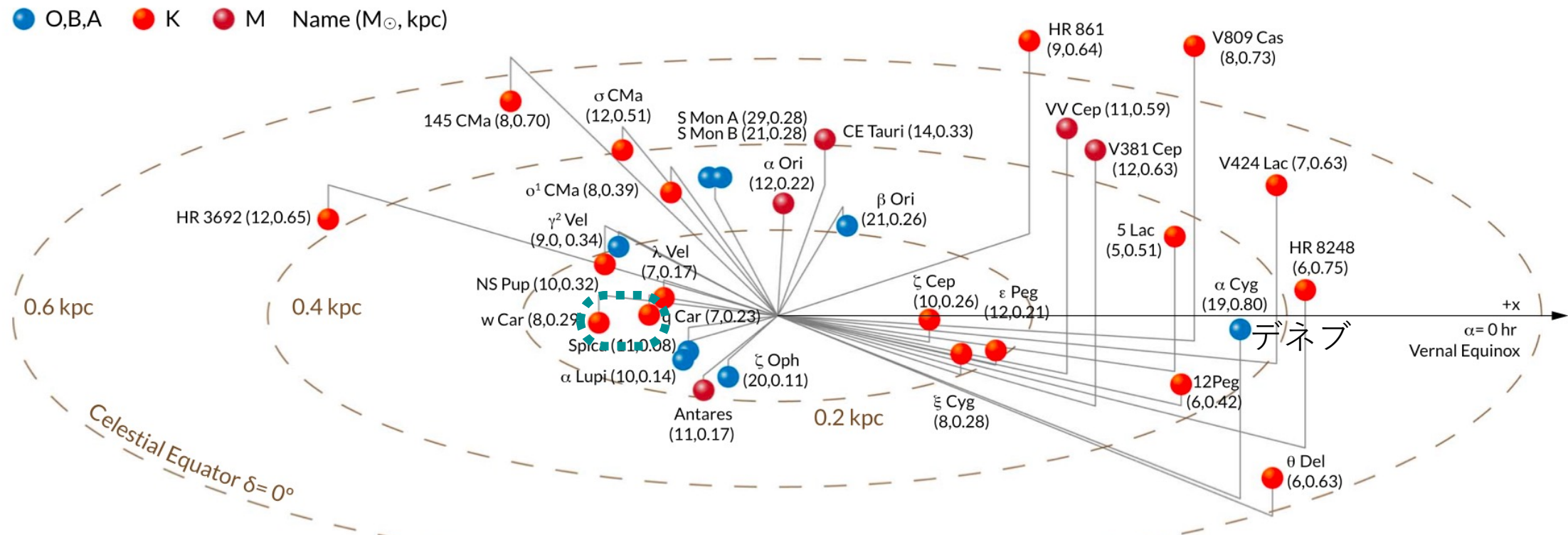


Figure 2. Illustration of nearby ($D \leq 1$ kpc) core collapse supernova candidates. Each star's spectral type, name, mass, and distance is shown in labels. See Table A1 for details and references.

Average minimum separation: 1.4 [deg]

70% of total candidates have their nearest neighborhood within 12.8 [deg]

Pre-SN candidates

Table A1 Mukhopadhyay, M., et al. *ApJ* 899.2 (2020): 153
Candidate Presupernova Stars

N	Catalog Name	Common Name	Constellation	Distance (kpc)	Mass (M_{\odot})	R.A.	Decl.
1	HD 116658	Spica/ α Virginis	Virgo	$0.077 \pm 0.004^{\text{a}}$	$11.43^{+1.15}_{-1.15}{}^{\text{b}}$	13:25:11.58	-11:09:40.8
2	HD 149757	ζ Ophiuchi	Ophiuchus	$0.112 \pm 0.002^{\text{a}}$	20.0 ^c	16:37:09.54	-10:34:01.53
3	HD 129056	α Lupi	Lupus	$0.143 \pm 0.003^{\text{a}}$	$10.1^{+1.0}_{-1.0}{}^{\text{d}}$	14:41:55.76	-47:23:17.52
4	HD 78647	λ Velorum	Vela	$0.167 \pm 0.003^{\text{a}}$	$7.0^{+1.5}_{-1.0}{}^{\text{e}}$	09:07:59.76	-43:25:57.3
5	HD 148478	Antares/ α Scorpii	Scorpius	$0.169 \pm 0.030^{\text{a}}$	$11.0 - 14.3^{\text{f}}$	16:29:24.46	-26:25:55.2
6	HD 206778	ϵ Pegasi	Pegasus	$0.211 \pm 0.006^{\text{a}}$	$11.7^{+0.8}_{-0.8}{}^{\text{d}}$	21:44:11.16	+09:52:30.0
7	HD 39801	Betelgeuse/ α Orionis	Orion	$0.222 \pm 0.040^{\text{r}}$	$11.6^{+5.0}_{-3.9}{}^{\text{g}}$	05:55:10.31	+07:24:25.4
8	HD 89388	q Car/V337 Car	Carina	$0.230 \pm 0.020^{\text{p}}$	$6.9^{+0.6}_{-0.6}{}^{\text{d}}$	10:17:04.98	-61:19:56.3
9	HD 210745	ζ Cephei	Cepheus	$0.256 \pm 0.006^{\text{p}}$	$10.1^{+0.1}_{-0.1}{}^{\text{d}}$	22:10:51.28	+58:12:04.5
10	HD 34085	Rigel/ β Orion	Orion	$0.264 \pm 0.024^{\text{a}}$	$21.0^{+3.0}_{-3.0}{}^{\text{h}}$	05:14:32.27	-08:12:05.90
11	HD 200905	ξ Cygni	Cygnus	$0.278 \pm 0.029^{\text{p}}$	8.0 ⁱ	21:04:55.86	+43:55:40.3
12	HD 47839	S Monocerotis A	Monoceros	$0.282 \pm 0.040^{\text{a}}$	29.1 ^j	06:40:58.66	+09:53:44.71
13	HD 47839	S Monocerotis B	Monoceros	$0.282 \pm 0.040^{\text{a}}$	21.3 ^j	06:40:58.57	+09:53:42.20
14	HD 93070	w Car/V520 Car	Carina	$0.294 \pm 0.023^{\text{p}}$	$7.9^{+0.1}_{-0.1}{}^{\text{d}}$	10:43:32.29	-60:33:59.8
15	HD 68553	NS Puppis	Puppis	$0.321 \pm 0.032^{\text{p}}$	9.7 ^d	08:11:21.49	-39:37:06.8
16	HD 36389	CE Tauri/119 Tauri	Taurus	$0.326 \pm 0.070^{\text{p}}$	$14.37^{+2.00}_{-2.77}{}^{\text{k}}$	05:32:12.75	+18:35:39.2
17	HD 68273	γ^2 Velorum	Vela	$0.342 \pm 0.035^{\text{a}}$	$9.0^{+0.6}_{-0.6}{}^{\text{l}}$	08:09:31.95	-47:20:11.71
18	HD 50877	σ^1 Canis Majoris	Canis Major	$0.394 \pm 0.052^{\text{p}}$	$7.83^{+2.0}_{-2.0}{}^{\text{d}}$	06:54:07.95	-24:11:03.2
19	HD 207089	12 Pegasi	Pegasus	$0.415 \pm 0.031^{\text{p}}$	$6.3^{+0.7}_{-0.7}{}^{\text{d}}$	21:46:04.36	+22:56:56.0
20	HD 213310	5 Lacertae	Lacerta	$0.505 \pm 0.046^{\text{a}}$	$5.11^{+0.18}_{-0.18}{}^{\text{m}}$	22:29:31.82	+47:42:24.8
21	HD 52877	σ Canis Majoris	Canis Major	$0.513 \pm 0.108^{\text{p}}$	$12.3^{+0.1}_{-0.1}{}^{\text{d}}$	07:01:43.15	-27:56:05.4
22	HD 208816	VV Cephei	Cepheus	$0.599 \pm 0.083^{\text{p}}$	$10.6^{+1.0}_{-1.0}{}^{\text{d}}$	21:56:39.14	+63:37:32.0
23	HD 196725	θ Delphini	Delphinus	$0.629 \pm 0.029^{\text{p}}$	$5.60^{+3.0}_{-3.0}{}^{\text{n}}$	20:38:43.99	+13:18:54.4
24	HD 203338	V381 Cephei	Cepheus	$0.631 \pm 0.086^{\text{p}}$	12.0 ^o	21:19:15.69	+58:37:24.6
25	HD 216946	V424 Lacertae	Lacerta	$0.634 \pm 0.075^{\text{p}}$	$6.8^{+1.0}_{-1.0}{}^{\text{q}}$	22:56:26.00	+49:44:00.8
26	HD 17958	HR 861	Cassiopeia	$0.639 \pm 0.039^{\text{p}}$	$9.2^{+0.5}_{-0.5}{}^{\text{d}}$	02:56:24.65	+64:19:56.8
27	HD 80108	HR 3692	Vela	$0.650 \pm 0.061^{\text{p}}$	$12.1^{+0.2}_{-0.2}{}^{\text{d}}$	09:16:23.03	-44:15:56.6
28	HD 56577	145 Canis Major	Canis Major	$0.697 \pm 0.078^{\text{p}}$	$7.8^{+0.5}_{-0.5}{}^{\text{d}}$	07:16:36.83	-23:18:56.1
29	HD 219978	V809 Cassiopeia	Cassiopeia	$0.730 \pm 0.074^{\text{p}}$	$8.3^{+0.5}_{-0.5}{}^{\text{d}}$	23:19:23.77	+62:44:23.2
30	HD 205349	HR 8248	Cygnus	$0.746 \pm 0.039^{\text{p}}$	$6.3^{+0.7}_{-0.7}{}^{\text{d}}$	21:33:17.88	+45:51:14.5
31	HD 102098	Deneb/ α Cygni	Cygnus	$0.802 \pm 0.066^{\text{s}}$	$19.0^{+4.0}_{-4.0}{}^{\text{s}}$	20:41:25.9	+45:16:49.0

Minimum Angular Separation between Pre-SN candidates

Table A2
Minimum Angular Separation between Presupernova Candidates
Mukhopadhyay, M., et al. *ApJ* 899.2 (2020): 153

N	Catalog/Common Name	Min. Ang. Separation (deg)	Nearest Neighbor Name	Nearest Neighbor Number
1	HD 116658/Spica	39.66	HD 129056/ α Lupi	3
2	HD 149757/ ζ Ophiuchi	15.97	HD 148478/Antares	5
3	HD 129056/ α Lupi	29.73	HD 148478/Antares	5
4	HD 78647/ λ Velorum	1.73	HD 80108/HR 3692	27
5	HD 148478/Antares	15.97	HD 149757/ ζ Ophiuchi	2
6	HD 206778/ ϵ Pegasi	13.08	HD 207089/12 Pegasi	19
7	HD 39801/Betelgeuse	11.59	S Mono A/B	12/13
8	HD 89338/q Car	3.30	HD 93070/w Car	14
9	HD 210745/ ζ Cephei	5.69	HD 208816/VV Cephei	22
10	HD 34085/Rigel	18.60	HD 39801/Betelgeuse	7
11	HD 200905/ ζ Cygni	4.39	HD 102098/Deneb	31
12	HD 47839/S Mono A	11.60	HD 39801/Betelgeuse	7
13	HD 47839/S Mono B	11.60	HD 39801/Betelgeuse	7
14	HD 93070/w Car	3.30	HD 89338/q Car	8
15	HD 68553/NS Puppis	7.72	HD 68273/ γ^2 Velorum	17
16	HD 36389/119 Tauri	12.50	HD 39801/Betelgeuse	7
17	HD 68273/ γ^2 Velorum	7.72	HD 68553/NS Puppis	15
18	HD 50877/ σ^1 Canis Majoris	4.12	HD 52877/ σ Canis Majoris	21
19	HD 207089/12 Pegasi	13.08	HD 206778/ ϵ Pegasi	6
20	HD 213310/5 Lacertae	4.88	HD 216946/V424 Lacertae	25
21	HD 52877/ σ Canis Majoris	4.12	HD 50877/ σ^1 Canis Majoris	18
22	HD 208816/VV Cephei	5.69	HD 210745/ ζ Cephei	9
23	HD 196725/ θ Delphini	16.39	HD 206778/ ϵ Pegasi	6
24	HD 203338/V381 Cephei	6.72	HD 208816/VV Cephei	22
25	HD 216946/V424 Lacertae	4.88	HD 213310/5 Lacertae	20
26	HD 17958/HR 861	23.49	HD 219978/V809 Cassiopeia	29
27	HD 80108/HR 3692	1.73	HD 78647/ λ Velorum	4
28	HD 56577/145 Canis Majoris	5.22	HD 50877/ σ^1 Canis Majoris	18
29	HD 219978/V809 Cassiopeia	9.33	HD 208816/VV Cephei	22
30	HD 205349/HR 8248	5.38	HD 200905/ ζ Cygni	11
31	HD 102098/Deneb	4.39	HD 200905/ ζ Cygni	11